© 2021. Published by The Company of Biologists Ltd | Development (2021) 148, dev194928. doi:10.1242/dev.194928

RESEARCH REPORT

TRPM7 is a crucial regulator of pancreatic endocrine development and high-fat-diet-induced β-cell proliferation

Molly K. Altman[1,*], Charles M. Schaub[1,*], Prasanna K. Dadi[1], Matthew T. Dickerson[1,‡], Karolina E. Zaborska[1,‡], Arya Y. Nakhe[1], Sarah M. Graff[1], Thomas J. Galletta[1], Gautami Amarnath[1,2], Ariel S. Thorson[1], Guoqiang Gu[3] and David A. Jacobson[1,§]

ABSTRACT

The melastatin subfamily of the transient receptor potential channels (TRPM) are regulators of pancreatic β-cell function. TRPM7 is the most abundant islet TRPM channel; however, the role of TRPM7 in β-cell function has not been determined. Here, we used various spatiotemporal transgenic mouse models to investigate how TRPM7 knockout influences pancreatic endocrine development, proliferation and function. Ablation of TRPM7 within pancreatic progenitors reduced pancreatic size, and α-cell and β-cell mass. This resulted in modestly impaired glucose tolerance. However, TRPM7 ablation following endocrine specification or in adult mice did not impact endocrine expansion or glucose tolerance. As TRPM7 regulates cell proliferation, we assessed how TRPM7 influences β-cell hyperplasia under insulin-resistant conditions. β-Cell proliferation induced by high-fat diet was significantly decreased in TRPM7-deficient β-cells. The endocrine roles of TRPM7 may be influenced by cation flux through the channel, and indeed we found that TRPM7 ablation altered β-cell Mg^{2+} and reduced the magnitude of elevation in β-cell Mg^{2+} during proliferation. Together, these findings revealed that TRPM7 controls pancreatic development and β-cell proliferation, which is likely due to regulation of Mg^{2+} homeostasis.

KEY WORDS: β-Cell proliferation, Insulin secretion, Islet development, Magnesium handling, TRPM7

INTRODUCTION

Although Mg^{2+} serves many essential roles and is the most abundant divalent cation in pancreatic β-cells, the mechanisms that modulate β-cell Mg^{2+} homeostasis have not been conclusively determined (Fang et al., 2013; Sahni and Scharenberg, 2008; Sahni et al., 2010; Sgambato et al., 1999; Yu et al., 2014). The transient receptor potential cation (TRPM) channel, TRPM7, is a regulator of cellular Mg^{2+} homeostasis and *TRPM7* is one of the most abundant TRPM transcripts expressed in human β-cells (Li et al., 2016a; Ryazanova et al., 2010; Schmitz et al., 2003). TRPM7 channels are inactivated at physiological Mg^{2+} levels and are activated in response to a decrease in intracellular or extracellular Mg^{2+}; thus, TRPM7 channels tightly control intracellular Mg^{2+} levels (Schmitz et al., 2003). For example, TRPM7 channels facilitate Mg^{2+} influx during the G1 phase of the cell cycle, which stimulates DNA and protein synthesis (Rubin, 2005b; Tani et al., 2007). TRPM7 is also essential for embryonic development, as silencing or deleting TRPM7 perturbs organogenesis (Jin et al., 2008, 2012). Furthermore, reduced TRPM7 expression results in decreased proliferation (Fang et al., 2013; Ryazanova et al., 2010; Sahni et al., 2010). Interestingly, Mg^{2+} supplementation restores cell cycle progression and organogenesis in the absence of TRPM7, which reinforces the importance of Mg^{2+} homeostasis during development (Ryazanova et al., 2010; Yee et al., 2005, 2011). Although it has been established that TRPM7 control of Mg^{2+} handling regulates cellular development and proliferation, the role of TRPM7 in β-cell function remains poorly understood.

TRPM7 control of Mg^{2+} regulates the expression and activity of cell cycle and signaling pathways that influence pancreatic-cell and β-cell proliferation (Fang et al., 2013; Sahni and Scharenberg, 2008; Sahni et al., 2010; Sgambato et al., 1999; Yee et al., 2011; Yu et al., 2014). TRPM7 knockdown (KD) in pancreatic adenocarcinoma cells (BxPC-3 and PANC-1) decreases proliferation owing to upregulation of $p21^{cip1}$ and suppressor of cytokine signaling 3a, which is restored by supplementation with high extracellular Mg^{2+} (Yee et al., 2011). In other cell types, TRPM7 ablation altered expression of key cell cycle regulatory proteins, many of which modulate β-cell development and proliferation (Fang et al., 2013; Sahni and Scharenberg, 2008; Sahni et al., 2010; Sgambato et al., 1999; Yu et al., 2014). For example, lymphocyte proliferation is decreased following TRPM7 ablation due in part to $p27^{Kip1}$ upregulation; similarly, overexpression of $p27^{Kip1}$ inhibits both neonatal and postnatal β-cell proliferation, whereas β-cell knockout (KO) of $p27^{Kip1}$ increases β-cell mass (Rachdi et al., 2006; Sahni et al., 2010). TRPM7 KD in hepatic cells reduces expression of G1 checkpoint regulators (cyclin D1 and Cdk4), both of which stimulate β-cell proliferation (Cozar-Castellano et al., 2004; Fang et al., 2013; Rane et al., 1999; Zhang et al., 2005). TRPM7 KO also resulted in decreased mTOR, AKT and ERK activity, which are crucial determinates of β-cell proliferation in response to a high fat diet (HFD), during pregnancy and in neonates (Alejandro et al., 2014; Balcazar et al., 2009; Bernal-Mizrachi et al., 2004, 2001; Chen et al., 2011; Fang et al., 2013; Gupta et al., 2007; Sahni and Scharenberg, 2008; Sahni et al., 2010; Sgambato et al., 1999; Yu et al., 2014). This suggests that TRPM7 channel modulation of pancreatic-cell Mg^{2+} handling may influence cell cycle progression and proliferative capacity.

Recent evidence has begun to reveal the importance of TRPM7 in maintaining Mg^{2+} homeostasis during pancreas development. A random mutagenesis screen in zebrafish found that TRPM7

[1]Department of Molecular Physiology and Biophysics, Vanderbilt University, 7425B MRB IV, 2213 Garland Ave., Nashville, TN 37232, USA. [2]Molecular Neurophysiology, Institute of Applied Physiology, University of Ulm, 89081 Ulm, Germany. [3]Vanderbilt Program in Developmental Biology, Vanderbilt Center for Stem Cell Biology, Department of Cell and Developmental Biology, Vanderbilt University School of Medicine, Nashville, TN 37232, USA.
*These authors contributed equally to this work
‡These authors contributed equally to this work

§Author for correspondence (david.a.jacobson@vanderbilt.edu)

C.M.S., 0000-0002-3251-3455; P.K.D., 0000-0001-5377-5991; M.T.D., 0000-0002-6187-3951; S.M.G., 0000-0001-9305-1760; D.A.J., 0000-0003-1816-5375

Handling Editor: Gordon Keller
Received 15 July 2020; Accepted 20 July 2021

Development (2021) 148, dev194928. doi:10.1242/dev.194928

inactivation reduces pancreas mass, a phenotype replicated by TRPM7 KD of zebrafish (Yee et al., 2005, 2011). Importantly, Mg^{2+} supplementation partially restores pancreatic size in TRPM7 KD zebrafish, which suggested that TRPM7 control of Mg^{2+} homeostasis is crucial for pancreas development (Yee et al., 2005, 2011). As TRPM7 is known to serve an important role in early organogenesis, it may impact pancreatic progenitor proliferation and/or function, which could affect the endocrine progenitor pool (Jin et al., 2012). Indeed, TRPM7 ablation in neural crest progenitors (NCPs) leads to loss of pigment cells and dorsal root ganglion neurons (Jin et al., 2012). Interestingly, ablation of NCP TRPM7 at embryonic day (E) 10.5, but not E14.5, disrupted development (Jin et al., 2012). Although this suggests that TRPM7 serves a function during early pancreas organogenesis, the role of TRPM7 in controlling development from either pancreatic or endocrine progenitors has not been established. Therefore, it is important to determine whether TRPM7 impacts pancreas organogenesis and endocrine specification during the specific progenitor developmental time points that determine endocrine mass.

In addition to its influence on pancreas development, Mg^{2+} flux through TRPM7 channels directly regulates β-cell function (Gommers et al., 2019). For example, glucose-stimulated insulin secretion (GSIS) from INS-1 rat insulinoma cells is enhanced following TRPM7 KD (Gommers et al., 2019). The changes in GSIS caused by TRPM7 are likely because of prolonged reductions in Mg^{2+} or mediated via its permeability to other divalent ions, such as Zn^{2+} or Ca^{2+} (Gommers et al., 2019). Zn^{2+} is crucial for insulin crystallization in granules; rodent β-cells expressing a loss-of-function Zn^{2+} transporter (ZnT8) display increased GSIS resembling INS-1 TRPM7 KD GSIS, whereas ZnT8 deletion results in decreased secretion (Hardy et al., 2012; Kleiner et al., 2018). Because TRPM7 is an outward-rectifying channel with only modest Ca^{2+} conductance at physiological membrane potentials (Runnels et al., 2001), it is unlikely that Ca^{2+} entry through TRPM7 channels would directly affect β-cell Ca^{2+} handling. However, TRPM7 channel control of intracellular Mg^{2+} could indirectly modulate β-cell Ca^{2+} handling by influencing voltage-dependent Ca^{2+} channel activity (Nguemo et al., 2014; Zierler et al., 2017). Thus, it is important to determine whether TRPM7 influences primary β-cell GSIS and whether this could be due to alterations in divalent cation flux.

Here, we show that TRPM7 serves important roles in pancreatic endocrine development and function. The data indicate that TRPM7 promotes early pancreatic endocrine development and β-cell proliferation. Furthermore, these findings identify that TRPM7 controls β-cell Mg^{2+} and Ca^{2+} handling, which could contribute to the enhanced GSIS observed in islets with TRPM7 ablation. Finally, the data reveal that TRPM7 contributes to elevating β-cell Mg^{2+} during proliferation.

RESULTS AND DISCUSSION

TRPM7 is a crucial determinant of pancreatic exocrine and endocrine development

TRPM7 is a key determinant of pancreas size in zebrafish and serves a crucial role during early organogenesis (Jin et al., 2012; Yee et al., 2005, 2011); therefore, we investigated the effect of TRPM7 on mouse pancreatic development. A mouse line with floxed *TRPM7* exon 17 ($TRPM7^{fl/fl}$) and a Pdx1-Cre^{TUV} transgene was used to selectively knockout TRPM7 in pancreatic progenitor cells (termed $TRPM7KO^{Panc}$); loss of TRPM7 protein expression in $TRPM7KO^{Panc}$ pancreata was confirmed following removal of *TRPM7* exon17 in islets (Fig. S1A-C). $TRPM7KO^{Panc}$ mice displayed pancreatic hypoplasia and reduced pancreatic mass at E16.5 compared with controls [35.6±8.5% reduction (mean ±s.e.m.), Fig. 1A-C; Fig. S2A]. Total pancreatic area was also reduced in $TRPM7KO^{Panc}$ mice compared with controls (59.4 ±20.1% decrease, Fig. 1F). These results indicate that TRPM7 channels are crucial mediators of mouse exocrine pancreatic development.

To determine the effect of TRPM7 ablation on pancreatic endocrine development, we compared β- and α-cell mass of control and $TRPM7KO^{Panc}$ mice (Fig. 1D-J). $TRPM7KO^{Panc}$ pancreata had fewer β-cells (31.2±10.8% decrease, Fig. 1G), reduced β-cell mass (55.8±9.9% decrease, Fig. 1H) and decreased total pancreatic insulin content (47.4±15.8% decrease, Fig. S2B) compared with controls. $TRPM7KO^{Panc}$ pancreata also had fewer α-cells (39.6 ±11.7% decrease, Fig. 1I) and decreased total α-cell mass (61.2 ±9.2% decrease, Fig. 1J) compared with controls. Intraperitoneal glucose tolerance tests (IPGTTs) were performed to assess the impact of reduced endocrine mass on glucose homeostasis. Despite a significant decrease in β-cell number (Fig. 1G), β-cell mass (Fig. 1H) and total insulin content (Fig. S2B), the $TRPM7KO^{Panc}$ mice were only modestly glucose intolerant compared with controls (Fig. 1K,L). Interestingly, isolated $TRPM7KO^{Panc}$ islets showed enhanced GSIS compared with controls (40.0±10.7% increase, Fig. S2C,D) even though total islet insulin content was decreased, which could potentially limit glucose intolerance in $TRPM7KO^{Panc}$ mice. Furthermore, although fasting plasma insulin was reduced in $TRPM7KO^{Panc}$ mice, plasma insulin reached control levels at 30 min post intraperitoneal (IP) glucose challenge (Fig. S2E). Also, the Pdx1-Cre^{TUV} line used for this study not only expresses cre in pancreatic progenitors but also in a limited number of other tissues such as the hypothalamus (Wicksteed et al., 2010); therefore, TRPM7 loss in other tissues may also impact glucose tolerance tests (GTT) in $TRPM7KO^{Panc}$ mice. Taken together, these data reveal that TRPM7 channels are key determinants of early pancreatic endocrine development.

Endocrine progenitor TRPM7 ablation does not alter endocrine mass or glucose homeostasis

Having identified a role for TRPM7 during early pancreatic organogenesis, we sought to determine whether TRPM7 is also required for endocrine progenitor differentiation. Although previous studies have found that TRPM7 is primarily a determinant of early organogenesis (Jin et al., 2012), it was important to confirm whether TRPM7 also serves a cell- or time-specific role during endocrine development. Therefore, an endocrine progenitor-selective TRPM7 ablation mouse was created by combining$TRPM7^{fl/fl}$ and Ngn3-Cre mice ($TRPM7KO^{Endo}$; Figs S1A and S3). There was no difference in β- and α-cell number, β- and α-cell area or pancreas area in $TRPM7KO^{Endo}$ pancreata compared with controls (Fig. 2A-G). This indicates that TRPM7 is not required for pancreatic development after endocrine progenitor specification. Moreover, $TRPM7KO^{Endo}$ mice showed equivalent glucose tolerance as controls (Fig. 2H,I males, Fig. S5A females). Although these findings suggest that the role of TRPM7 during pancreatic development is restricted to pancreatic progenitors, it is possible that TRPM7 has additional functions in mature islet cells (Gommers et al., 2019).

β-Cell TRPM7 ablation reduced HFD-induced proliferation but did not alter glucose tolerance

As TRPM7 regulates cell cycle and signaling pathways that influence β-cell proliferation (Chen et al., 2011; Fang et al., 2013; Sahni and Scharenberg, 2008; Sahni et al., 2010), TRPM7 control

Development (2021) 148, dev194928. doi:10.1242/dev.194928

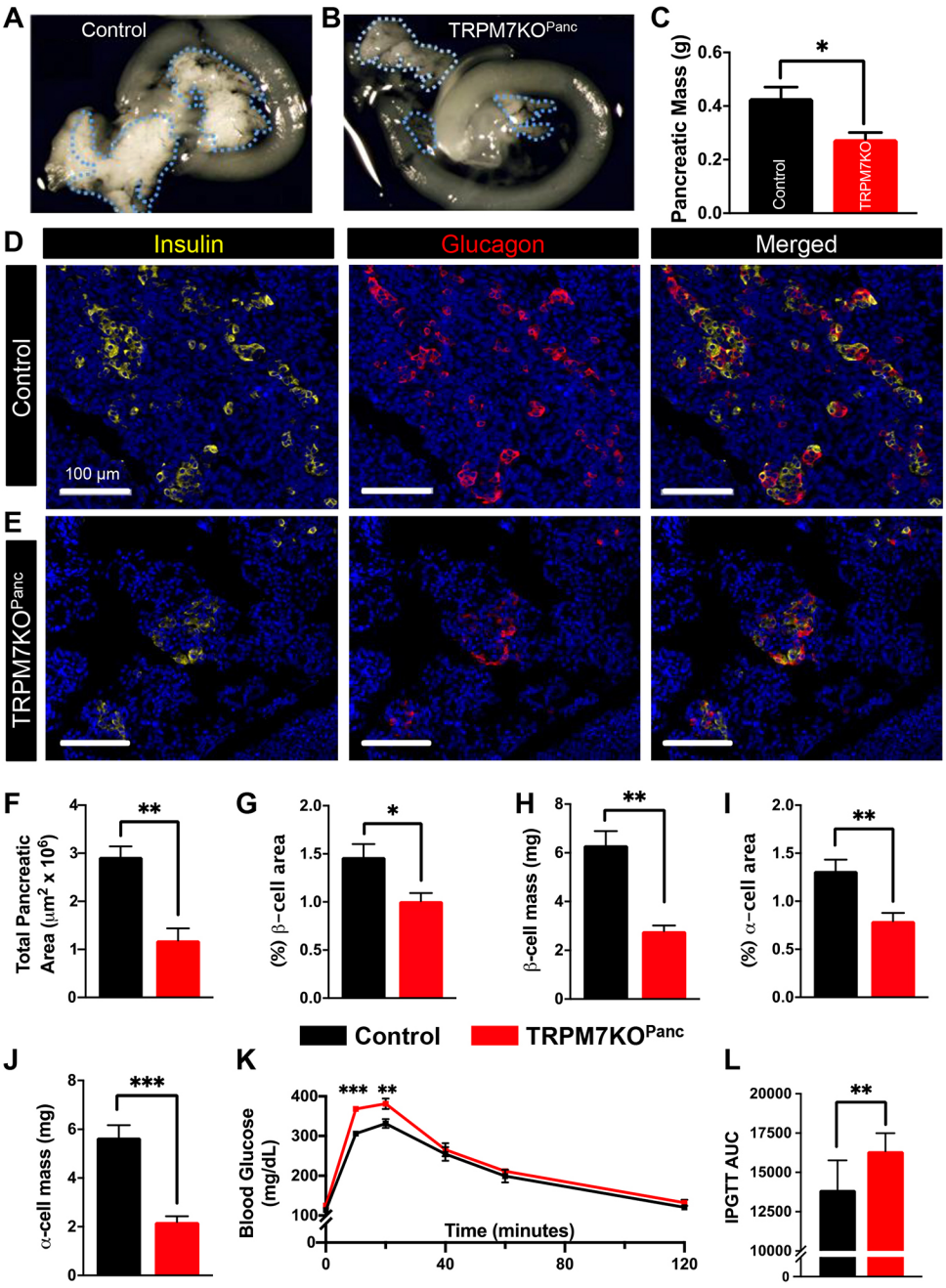

Fig. 1. TRPM7 ablation in pancreatic progenitors resulted in exocrine and endocrine hypoplasia and glucose intolerance. (A,B) Representative images of E16.5 pancreata (dotted blue lines) from control (A) and TRPM7KO^{Panc} (B) mice. (C) Pancreatic weight from control and TRPM7KO^{Panc} mice (n=4). (D,E) Pancreatic sections from control (D) and TRPM7KO^{Panc} (E) stained for insulin (yellow), glucagon (red) and nuclei (blue). Scale bars: 100 µm. (F-J) Total pancreatic area (E16.5) (F), β-cell area (G), β-cell mass (H), α-cell area (I) and α-cell mass (J) (controls: n=4; TRPM7KO^{Panc}: β-cells n=4, α-cells n=5) calculated relative to total pancreatic tissue. (K,L) Glucose tolerance (K) and corresponding AUC (L) (control: n=10; TRPM7KO^{Panc}: n=7). Analysis is relative to total pancreatic tissue with 10 sections analyzed per animal. Data are mean±s.e.m. *P<0.05; **P<0.01; ***P<0.001 (two-tailed unpaired Student's t-test).

of β-cell proliferation was investigated. Mice with conditional β-cell ablation of TRPM7 were placed on a HFD to examine the role of TRPM7 during HFD-induced β-cell proliferation; this mouse line contains both TRPM7$^{fl/fl}$ and *Ins1*^{CreERT2}(TRPM7KO^{INSβ}). Twelve-week-old TRPM7KO^{INSβ} mice or controls (*Ins1*^{CreERT2}) were treated with tamoxifen, allowed to recover for 2 weeks, placed on a HFD for 2 weeks, and then β-cell proliferation (Ki67^{+}) or apoptosis (TUNEL) were assessed. We found that β-cell proliferation was significantly reduced in TRPM7KO^{INSβ} pancreatic sections compared with control sections (47.9±12.0% decrease, Fig. 3A-C); TRPM7 KO did not affect β-cell apoptosis (Fig. S4A,B). Interestingly, although β-cell proliferation was reduced in TRPM7KO^{INSβ} sections compared with controls, total pancreatic area (Fig. 3D), islets per section (Fig. 3E) and average islet area were indistinguishable (Fig. 3F). In addition, there was no difference in glucose tolerance pre- or post-HFD in TRPM7KO^{INSβ} animals compared with controls (Fig. 3G-J males, Fig. S5B females). Based on these findings, TRPM7 regulates HFD-induced β-cell proliferation but does not alter glucose tolerance.

TRPM7 enhanced elevations in β-cell Mg^{2+} influx during proliferation

TRPM7 control of Mg^{2+} has been shown to regulate pancreatic mass in zebrafish and proliferation in numerous cell types (Fang et al., 2013; Ryazanova et al., 2010; Sahni et al., 2010; Yee et al., 2005, 2011). Therefore, we explored whether TRPM7KO^{Panc} and/or TRPM7KO^{INSβ} β-cells have altered Mg^{2+} handling. Some studies also used another conditional β-cell TRPM7 KO mouse line (TRPM7$^{fl/fl}$ crossed with MIP-Cre/ERT, termed TRPM7KO^{MIPβ}; Fig. S6A). First, TRPM7 channels were activated by removing

Development (2021) 148, dev194928. doi:10.1242/dev.194928

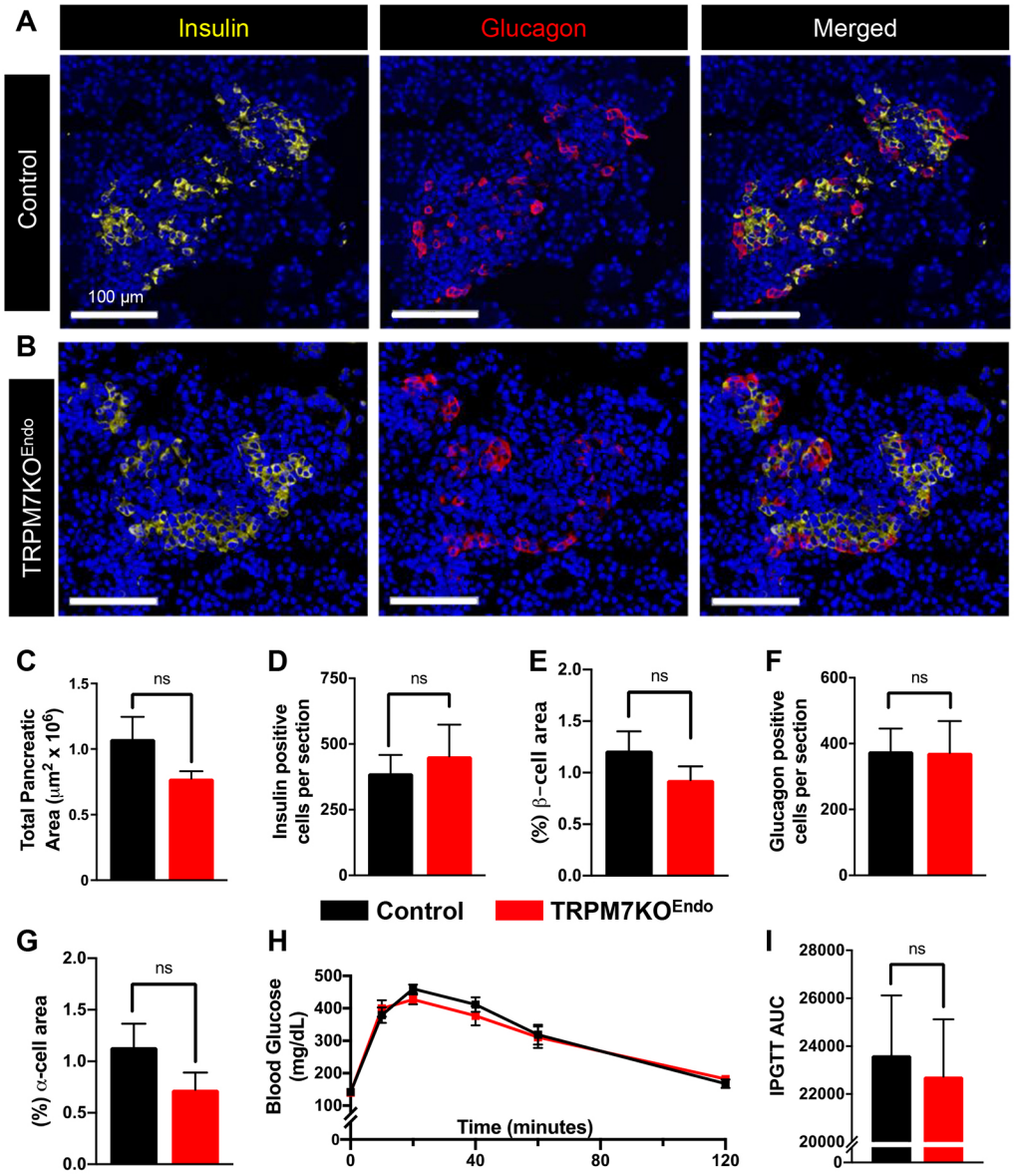

Fig. 2. TRPM7 ablation in endocrine progenitors did not impact α- and β-cell mass or glucose tolerance. (A,B) Immunostaining of pancreatic sections from control (A) and TRPM7KO^{Endo} (B) for insulin (yellow), glucagon (red) and nuclei (blue). Scale bars: 100 µm. (C) Total pancreatic area (E16.5) of control and TRPM7KO^{Endo} mice (n=3, P=0.165). (D,E) Total β-cell number per section (D; control: n=5; TRPM7KO^{Endo}: n=3) and β-cell area per animal (E; n=5, P=0.242). (F,G) Total α-cell number per section (F; control: n=5; TRPM7KO^{Endo}: n=3) and α-cell area per animal (G; n=5, P=0.178). (H,I) GTT (H) and corresponding AUC (I) (control: n=5; TRPM7KO^{Endo}: n=4). Analysis is relative to total pancreatic tissue with 10 sections analyzed per animal. Data are mean±s.e.m. ns, not significant.

extracellular divalent cations and β-cell TRPM7 currents measured in response to a voltage ramp from −120 mV to +60 mV (Fig. 4A; Fig. S7A,B). TRPM7 currents were significantly reduced under hyperpolarized (−120 to −65 mV) and depolarized (+25 to +60 mV) conditions in TRPM7KO^{Panc} β-cells compared with controls (Fig. 4A; Fig. S7A,B). Next, intracellular Mg^{2+} was monitored in TRPM7KO^{Panc}, TRPM7KO^{INSβ} and TRPM7KO^{MIPβ} β-cells; following removal of extracellular Mg^{2+}, intracellular Mg^{2+} levels were elevated in TRPM7 KO β-cells relative to controls (Fig. 4B,C,D; Fig. S8A). As TRPM7 modulation of Mg^{2+} homeostasis regulates cell proliferation in other tissues (Tani et al., 2007), we sought to determine whether this is the case in β-cells. Thus, cytosolic Mg^{2+} was quantified in proliferating (squares, Ki67-positive) and non-proliferating (circles, Ki67-negative) β-cells (Fig. 4C,D). Intracellular Mg^{2+} was elevated in non-proliferating TRPM7KO^{INSβ} single β-cells and also in β-cells within clusters of islet cells (Fig. 4C,D; Fig. S9A,B). Proliferating β-cells from TRPM7KO^{INSβ} and controls have significantly elevated intracellular Mg^{2+} when normalized to non-proliferating control cells (21.4±3.9% and 29.4±3.4% increase, respectively, Fig. 4E; Fig. S9C). However, as the non-proliferating TRPM7KO^{INSβ} β-cells had greater basal Mg^{2+}, the associated magnitude of elevation in Mg^{2+} during proliferation was reduced in TRPM7KO^{INSβ} compared with controls (48.5±17.9% decrease, Fig. 4F), presumably owing to loss of TRPM7. Furthermore, TRPM7 KO resulted in decreased β-cell proliferation (53.3±19.1% decrease, Fig. S9D), which is consistent with intact pancreatic sections (Fig. 3C). This suggests that TRPM7 limits non-proliferating β-cell Mg^{2+} levels; thus, during proliferation β-cells undergo a greater magnitude in elevation of intracellular Mg^{2+} when TRPM7 is active, which may promote proliferation.

β-Cell TRPM7 limited insulin secretion in a Ca^{2+}-independent manner

In addition to Mg^{2+}, TRPM7 channels are permeable to other divalent cations, thus we examined whether entry of Zn^{2+} or Ca^{2+} though TRPM7 channels may contribute to the enhanced GSIS observed in TRPM7 KD INS-1 cells (Gommers et al., 2019). First, we confirmed whether TRPM7KO^{MIPβ} islets show enhanced GSIS. Although insulin secretion from TRPM7KO^{MIPβ} islets was indistinguishable

Development (2021) 148, dev194928. doi:10.1242/dev.194928

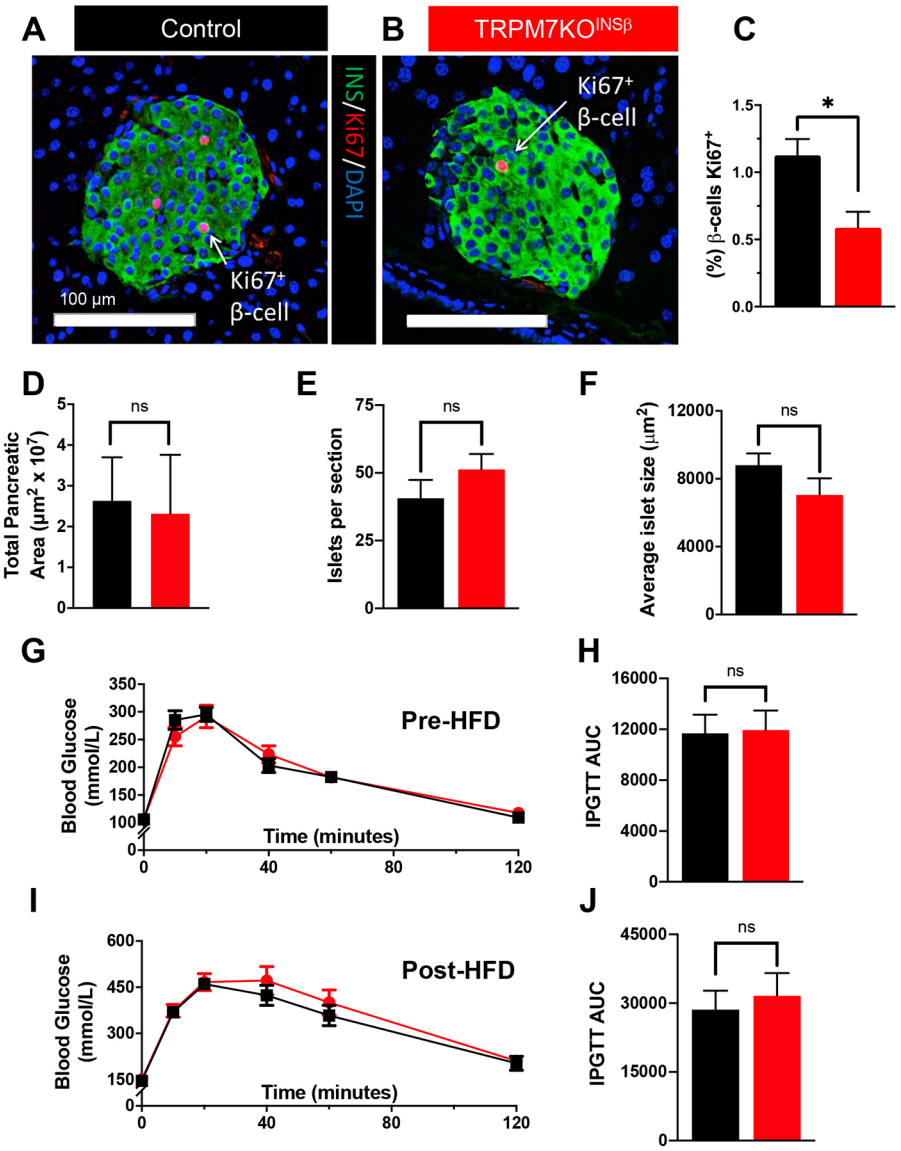

Fig. 3. β-Cell-specific TRPM7 ablation reduced HFD-induced β-cell proliferation. (A,B) Representative images of pancreatic islets from control (A) and TRPM7KO^{INSβ} (B) immunostained for insulin (green) and the proliferation marker Ki67 (red) and nuclei (blue) post-HFD. Scale bars: 100 µm. (C-F) Percent of Ki67-positive β-cells (n=6) (C), total pancreatic area (n=4) (D), islets per section (control: n=9; TRPM7KO^{INSβ}: n=7) (E) and average islet area (control: n=9; TRPM7KO^{INSβ}: n=7) (F). (G-J) TRPM7KO^{Insβ} (n=11) and control (n=10) mice GTT pre-HFD (G,H) and post-HFD (I,J; n=10). Data are mean±s.e.m. *P<0.05 (two-tailed unpaired Student's t-test). ns, not significant.

from control islets under euglycemic (7 mM glucose) conditions, GSIS (14 mM glucose) was increased compared with controls (73.7 ±16.0% increase, Fig. S6C). In the presence of elevated extracellular Zn^{2+}, the rate of cytosolic Zn^{2+} accumulation in TRPM7KO^{MIPβ} β-cells was indistinguishable from controls (Fig. S8B). This indicates that the minimal Zn^{2+} conductance through TRPM7 channels in β-cells is likely not important to their function. However, glucose-stimulated (14 mM) Ca^{2+} influx was decreased in TRPM7KO^{Panc} islets compared with controls (24.1±0.6% decrease, Fig. S2F,G). To determine whether TRPM7 channel-mediated enhancement of β-cell intracellular Ca^{2+} concentration ($[Ca^{2+}]_i$) was due to developmental changes in TRPM7KO^{Panc} β-cells, glucose-stimulated Ca^{2+} influx into TRPM7KO^{MIPβ} islets was also measured. Similar to total pancreatic TRPM7 channel ablation, glucose-stimulated Ca^{2+} influx was reduced in TRPM7KO^{MIPβ} islets compared with controls (Fig. S8C,D). As these data show that TRPM7 channels augment β-cell glucose-stimulated Ca^{2+} influx, it is unlikely that increased GSIS from TRPM7 KD INS-1 cells, or from TRPM7KO^{MIPβ} and TRPM7KO^{Panc} islets, is due to TRPM7 control of β-cell $[Ca^{2+}]_i$ (Gommers et al., 2019). However, as the frequency and amplitude of β-cell Ca^{2+} oscillations were not measured, TRPM7 modulation of GSIS by altering the kinetics of Ca^{2+} oscillations cannot be ruled out (Vierra et al., 2015). The change in GSIS is likely compensated for as TRPM7KO^{MIPβ} and control mice have equivalent glucose tolerance (Fig. S6B). Taken together, these data suggest that TRPM7 channels limit islet GSIS in addition to regulating β-cell development and proliferation.

Here, we show for the first time that TRPM7 regulates β-cell proliferation and GSIS, presumably by controlling β-cell Mg^{2+} homeostasis. Our findings indicate that β-cell intracellular Mg^{2+} levels increase during HFD-induced proliferation, as is the case in many other cell types (Fang et al., 2013; Rubin, 2005a; Sahni and Scharenberg, 2008; Sahni et al., 2010; Sgambato et al., 1999; Yee et al., 2011; Yu et al., 2014). Importantly, there was a significantly greater magnitude in elevation of intracellular Mg^{2+} during β-cell proliferation with functional TRPM7 channels, which is likely due to TRPM7 limiting intracellular Mg^{2+} levels in non-proliferating β-cells. This suggests that TRPM7-mediated control of Mg^{2+} homeostasis could play a role in β-cell proliferation (Tani et al., 2007). Moreover, reduced intracellular Mg^{2+} in non-proliferating β-cells with functional TRPM7 channels also indicates that TRPM7 regulates basal β-cell Mg^{2+} homeostasis. Although the exact

Development (2021) 148, dev194928. doi:10.1242/dev.194928

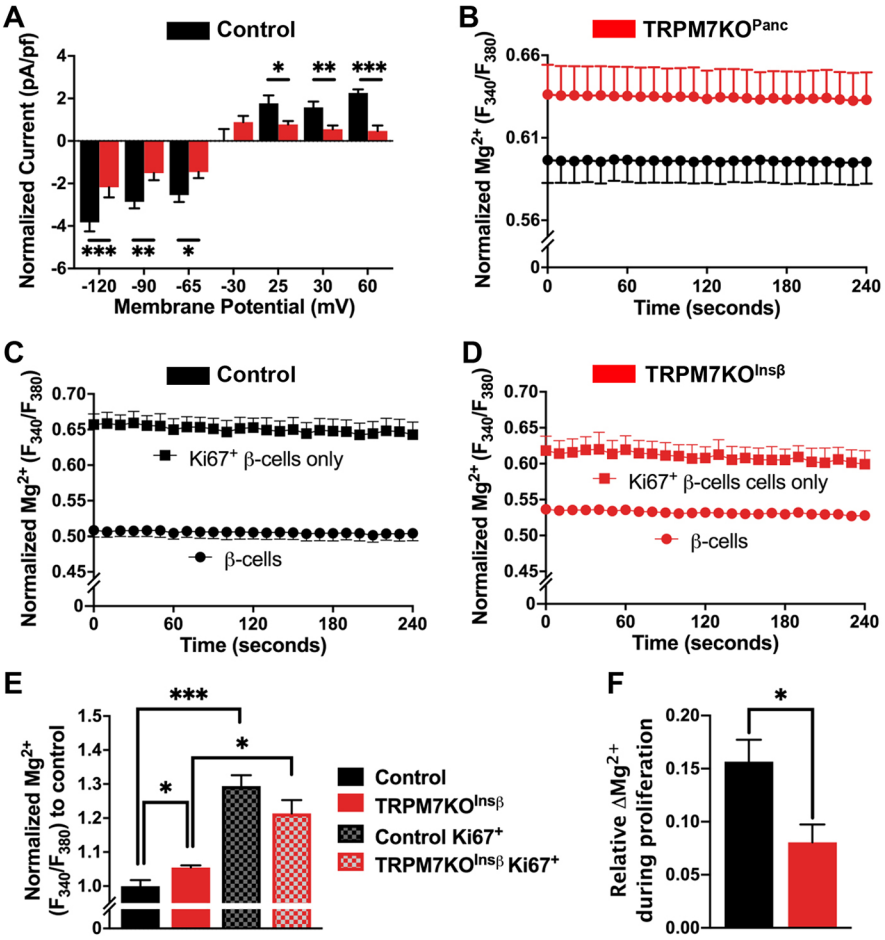

Fig. 4. TRPM7 enhanced β-cell divalent cation flux and controlled Mg^{2+} homeostasis. (A) TRPM7 current density from control (black, *n*=8) and TRPM7KO^{Panc} (red, *n*=7) β-cells at specified voltages. (B) Relative Mg^{2+} in control and TRPM7KO^{Panc} islets (*n*=4). (C,D) Mg^{2+} levels in dispersed non-proliferating (circles) and proliferating (squares) single β-cells from HFD-fed (2-week) control (C) and TRPM7KO^{Insβ} (D) mice. (E) Fold change in Mg^{2+} levels normalized to HFD-fed (2-week) non-proliferating controls. (F) Magnitude of intracellular Mg^{2+} increase during proliferation. Data are mean±s.e.m. **P*<0.05; ***P*<0.01; ****P*<0.001 (two-tailed unpaired Student's *t*-test).

mechanism(s) of how an elevation in cytosolic Mg^{2+} modulates β-cell proliferation remain(s) to be determined, in other cells Mg^{2+} influx can activate phosphoinositide 3-kinase-dependent signaling and AKT phosphorylation (Peng et al., 2020; Tuttle et al., 2001). Because AKT signaling is known to play a crucial role in β-cell proliferation (Peng et al., 2020; Tuttle et al., 2001), one possibility is that blunted AKT phosphorylation during proliferation in TRPM7-deficient β-cells limits proliferation in response to HFD. Perturbed Mg^{2+} homeostasis in TRPM7-deficient β-cells may impact other cell cycle pathways controlled by Mg^{2+} such as CDK2 kinase activity, expression of kinase inhibitor genes (e.g. $p21^{cip1}$ and $p27^{kip1}$), DNA synthesis and/or cytoskeletal remodeling (Harper et al., 1993; Polyak et al., 1994; Rubin, 1975). Finally, it has been shown that lymphocytes without TRPM7 channels enter a quiescent state, potentially owing to a large reduction in aerobic glycolysis necessary for sustained proliferation (Sahni et al., 2010). As Mg^{2+} is required for sequential enzymatic reactions within the glycolytic pathway, this may limit proliferation in TRPM7KO^{Insβ} β-cells under stressful conditions (Garfinkel and Garfinkel, 1985; Matsuda et al., 1999; Sahni and Scharenberg, 2008; Wimhurst and Manchester, 1972). Future studies are required to understand exactly how TRPM7 increases β-cell proliferation and how elevations in β-cell Mg^{2+} impact proliferation.

TRPM7 control of Mg^{2+} plays a crucial role in zebrafish pancreatic development and may also impact endocrine development. Indeed, the role of TRPM7 in endocrine cell development is striking, as TRPM7 KO in pancreatic progenitors resulted in >60% reduction of α- and β-cell mass (Fig. 1H,J). During early pancreatic development there is a large expansion of the multipotent progenitor cells, which are crucial determinants of adult pancreatic size (Stanger et al., 2007). Thus, TRPM7 may regulate the pool size of pancreatic progenitors, presumably through Mg^{2+} homeostasis that potentially regulates proliferation. Indeed, pancreatic development in TRPM7 KD zebrafish is rescued by Mg^{2+} supplementation (Yee et al., 2011). Therefore, future studies are needed to determine how Mg^{2+} alters pancreatic progenitor function as well as proliferation, and whether this is altered under conditions of aberrant Mg^{2+} handling during gestation. Conversely, there are no observed deleterious effects on endocrine mass or glucose tolerance following loss of TRPM7 during endocrine progenitor specification. Therefore, TRPM7 control of Mg^{2+} is likely not a crucial factor in endocrine differentiation (Castiglioni et al., 2013; Wang et al., 2010). This temporal developmental effect of TRPM7 is supported by studies on neural, kidney and pigment cells, in which TRPM7 is crucial for early organogenesis, but has a minimal effect on terminal differentiation (Jin et al., 2012). Taken together, our data indicate that TRPM7 plays an essential role in early pancreatic development as well as HFD-induced β-cell proliferation, which may be due in-part to TRPM7 control of Mg^{2+} handling. Therefore, these findings reveal that targeting TRPM7 or developing methods to control β-cell Mg^{2+} handling could provide therapeutic strategies for increasing β-cell mass.

MATERIALS AND METHODS

Mouse models

All mice used in these studies were 12-19 weeks old or harvested at E16.5, age-matched males on a C57BL/6 background. Animals were handled in

Development (2021) 148, dev194928. doi:10.1242/dev.194928

compliance with guidelines approved by the Vanderbilt University Animal Care and Use Committee protocols (protocol M1600063-01).

For spatiotemporal TRPM7 ablation, transgenic animals were used by crossing 129S4/SvJae mice containing LoxP sites inserted around exon 17 in the *TRPM7* gene (TRPM7$^{fl/fl}$, The Jackson Laboratory, 018784) (Jin et al., 2008) with various Cre-recombinase lines. For pancreatic progenitor-specific ablation, TRPM7$^{fl/fl}$ mice were crossed with C57BL/6 mice expressing a Cre-recombinase under the *Pdx1* promoter (Pdx1-cre)Tuv/J (Jin et al., 2008). Endocrine-specific ablation mice were created by crossing TRPM7$^{fl/fl}$ mice with Ngn3-cre mice (Gu et al., 2002). β-Cell-specific TRPM7 ablation mice were generated by crossing TRPM7$^{fl/fl}$ and C57BL/6 mice expressing a tamoxifen-activated CreERT-recombinase in β-cells (MIP-CreERT, the Jackson Laboratory, 024709; Ins1^{CreERT2}, the Jackson Laboratory, 026802) (Thorens et al., 2015; Wicksteed et al., 2010). Translocation of the CreERT into the nucleus was induced by treating CreERT mice with tamoxifen (2 mg ml^{-1}; RPI) every other day five times as indicated. Age-matched TRPM7$^{fl-/fl-}$ mice were used as controls and were treated with tamoxifen identically to the TRPM7$^{fl/fl}$ MIP-CreERT and TRPM7$^{fl/fl}$-*Ins1*^{CreERT2} mice.

Mouse diets and glucose tolerance testing

Mice were placed either on a normal chow or HFD (60% kcal from fat, D12492 Research Diets) and monitored for glucose tolerance. The GTT was performed as described previously by injecting 2 mg/kg dextrose and monitoring blood glucose at the indicated time points post-glucose injection after an ∼5-6 h fast (Jacobson et al., 2007). GTT was performed between 12-19 weeks of age and also in a cohort of mice placed on HFD for 2 weeks at 15 weeks of age.

Mouse islet and β-cell isolation

Mouse islets were isolated by digesting the pancreas with collagenase P (Roche) and performing density gradient centrifugation as previously described (Roe et al., 1994). Islets were plated or dissociated in 0.005% trypsin, placed on glass coverslips and cultured for 16 h in RPMI 1640 medium supplemented with 15% fetal bovine serum, specified glucose concentrations, 100 mg ml^{-1} penicillin, and 100 mg ml^{-1} streptomycin. Dissociated β-cells were used in all voltage clamp experiments recording Mg^{2+} currents. β-Cells on the periphery of intact islets were recorded in current clamp mode in all membrane potential recordings. Cells and islets were maintained in a humidified incubator at 37°C under an atmosphere of 95% air and 5% CO_2.

Islet insulin secretion assay

Insulin secretion from mouse islets was determined as previously described (Dadi et al., 2014). In summary, mouse islets were allowed to recover following isolation overnight at 5.6 mM glucose. For technical replicates, 20 equal-sized islets were incubated in 2 mM glucose in Krebs-Ringer buffer (KRB; 119 mM NaCl, 2 mM $CaCl_2$, 4.7 mM KCl, 10 mM HEPES, 1.2 mM $MgSO_4$, 1.2 mM KH_2PO_4, adjusted to pH 7.35 with NaOH) for 1 h, followed by the indicated treatments. Insulin concentrations were determined using the Insulin Rodent Chemiluminescence ELISA kit (ALPCO).

Whole cell voltage clamp electrophysiological recordings

TRPM7KO^{Panc} islets were dispersed into single cells and cultured overnight at 37°C, 5% CO_2. Recording pipettes (8-10 MΩ) were backfilled with intracellular solution containing (mM): 140.0 CsCl, 1.0 $MgCl_2$, 10.0 EGTA and 10.0 HEPES (pH 7.2, adjusted with CsOH) supplemented with 3.7 Mg-ATP. Cells were patched in extracellular buffer containing (mM): 119.0 NaCl, 4.7 KCl, 25.0 HEPES, 1.2 $MgSO_4$, 1.2 KH_2PO_4, 2.0 $CaCl_2$, (pH 7.4, adjusted with NaOH) supplemented with 14 mM glucose. After a whole-cell configuration was established (seal resistance>1 GΩ) the bath solution was exchanged (3 min) for divalent cation-free buffer containing (mM): 119.0 NaCl, 4.7 KCl, 25.0 HEPES, 1.2 KH_2PO_4 and 10.0 tetraethylammonium chloride supplemented with 14 mM glucose (pH 7.4, adjusted with NaOH). A voltage-clamp protocol was employed to record whole-cell currents with and without extracellular divalent cations in response to a voltage ramp from −120 to 60 mV (1 s interval) using an Axopatch 200B amplifier with pCLAMP10 software (Molecular Devices) as previously described (Vierra et al., 2015, 2017). TRPM7 currents were calculated by subtracting currents without divalents from currents with divalents. Data were analyzed using Clampfit 10 (Molecular Devices) and Microsoft Excel software.

Measurement of cytoplasmic Ca^{2+} and Zn^{2+}

Islet cell clusters were incubated (25 min at 37°C) in RPMI supplemented with 2 µM Fura-2 acetoxymethyl ester (Ca^{2+}) or 2 µM FluoZin-3 acetoxymethyl ester (Zn^{2+}; Molecular Probes). Fluorescence imaging was performed using a Nikon Eclipse TE2000-U microscope equipped with an epifluorescence illuminator (SUTTER), a CCD camera (HQ2, Photometrics) and Nikon Elements software. Relative Ca^{2+} concentrations were recorded with perifusion of KRB containing the indicated glucose concentrations and quantified every 5 s by determining the ratio of emitted fluorescence intensities at excitation wavelengths of 340 and 380 nm (F_{340}/F_{380}). The relative Ca^{2+} is plotted as the mean FURA-2 ratio (F_{340}/F_{380}) of each experimental group±s.e.m. Zn^{2+} concentrations were recorded with perifusion of KRB containing the indicated glucose and Zn^{2+} concentrations and quantified every 5 s by measuring the emitted fluorescent intensity at excitation of 516 nm and normalized to the lowest intensity per replicate. The averaged area under the curve (AUC) measurement for FURA-2 ratios and normalized FluoZin-3 levels during the indicated time period (min) was plotted as a bar graph. Data were analyzed using Excel and GraphPad Prism software and compared using an unpaired two-tailed Student's *t*-test.

Measurement of cytoplasmic Mg^{2+}

Islet cell clusters or dispersed β-cells were incubated (35 min at 37°C) in RPMI supplemented with ratiometric intracellular Mg^{2+} indicator Mag-fura-2 AM. This acetoxymethyl (AM) ester form was used for noninvasive intracellular loading (Invitrogen, M1292). Islet clusters or dispersed cells were washed three times with KRB-based solution without Mg^{2+} and then pre-incubated for 25-30 min before imaging. Fluorescence imaging and analysis of data were performed on a Nikon Eclipse scope and quantified every 5 s by measuring the emitted fluorescent intensity at excitation wavelengths of 340 and 380 nm (F_{340}/F_{380}) of each experimental group. Mg^{2+} monitored cells were then fixed with 4% paraformaldehyde and immunostained with primary antibodies: guinea pig anti-insulin (1:300; Millipore, 4011-01F; Hogh et al., 2013) and rabbit anti-Ki67 (1:300; Abcam, ab15580; Ji et al., 2019) and fluorescent isothiocyanate-conjugated secondary antibodies (1:300; Jackson ImmunoResearch) to identify Ki67^{+} β-cells.

Plasma insulin measurements

Animals were starved for ∼4 h before glucose injections and then blood was collected for insulin measurements. Blood was collected in EDTA-Heparin coated VAT tubes (Sarstedt). VAT Tubes were spun down with centrifugation at 10,000 RPM (∼9,400 ***g***) for 10 min at 4°C and serum supernatants were collected. Serum samples were determined by the Vanderbilt Hormone Assay and Analytical Services Core using an Insulin radioimmunoassay kit (Sigma-Aldrich).

Tissue preparation and histology

Pancreatic tissue was dissected and fixed overnight at 4°C in 4% paraformaldehyde, paraffin embedded and cut into 5-µm sections using a microtome (HM 355S, Thermo Fisher Scientific). Sections were incubated overnight with primary antibodies at 4°C followed by 1 h incubation in fluorescent isothiocyanate-conjugated secondary antibodies (1:300; Jackson ImmunoResearch) and DAPI nuclear stain (Invitrogen). Primary antibodies used were: guinea pig anti-insulin (1:300; Millipore, 4011-01F), rabbit anti-glucagon (1:300; Sigma-Aldrich, SAB4501137; Li et al., 2016b), rabbit anti-Ki67 (1:300; Abcam, ab15580) and mouse anti-cre (1:300; Sigma-Aldrich, MAB3120; Jeanes et al., 2012).

Analysis of endocrine cell mass

Measurements were carried out according to the protocol described by Henley et al. (2012). Briefly, 10 immunostained sections ∼250 µm apart (10

per animal) were visualized on an Aperio ScanScope FL and a custom macro for the ImageScope software was used to measure total pancreatic, β-cell and α-cell area (Rodriguez-Calvo et al., 2017). β-Cell mass was calculated using the ratio of β-cell area to total pancreas area of all sections for each animal and multiplied by the tissue wet weight.

Immunoprecipitation of TRPM7

Whole pancreas lysates from adult C57BL/6J and TRPM7KO^{Panc} were extracted and homogenized with a manual Potter-Elvehjem Tissue Homogenizer in RIPA buffer. Equal concentrations of extracts, as determined by BCA Protein Assay (Pierce), were then incubated overnight with mouse anti-TRPM7 (1:10; NeuroMab, 73-114) at 4°C, followed by an incubation with Protein A/G magnetic beads (Pierce). Bound protein was eluted according to the manufacturer's protocol. Eluted protein was run on a 10% SDS-Page Gel (Bio-Rad), followed by transfer to a nitrocellulose membrane. The blot was probed with rabbit anti-TRPM7 (1:1000; Sigma-Aldrich, PA5-15302) antibody and visualized with anti-rabbit conjugated to HRP antibody (1:1000; Promega, W401B) using SuperSignal West PicoPlus (Pierce).

Statistical analysis

All data were analyzed using Excel and GraphPad Prism software (v. 8.01). Statistical analysis for AUC, endocrine mass, proliferation and TUNEL was analyzed using a two-tailed unpaired Student's *t*-test using GraphPad Prism. Each *n* represents an individual animal and *n* values for all experiments are listed in the figure legends. A value of $P \leq 0.05$ was considered statistically significant.

Acknowledgements

We thank Maureen Gannon, Karin Bosma and Peter Kropp (Vanderbilt University Medical Center) for providing discussion and helpful suggestions regarding analysis and quantification of endocrine development as well as the CRE antibody. We thank Sonia Srikanth (Vanderbilt University) for taking pictures of some of the pancreatic sections. We thank the Vanderbilt Hormone Assay Core (supported by National Institutes of Health Grants DK-059637 and DK-020593) for performing insulin secretion immunoassays. We also thank the Vanderbilt Cell Imaging Shared Resource (CISR) for the confocal microscopes used for some of the images included in this manuscript (supported by National Institutes of Health grants DK-58404, C-68485, EY-08126 and DK-59637).

Competing interests

The authors declare no competing or financial interests.

Author contributions

Conceptualization: M.K.A., D.A.J.; Methodology: M.K.A., C.M.S., P.K.D., K.E.Z., M.T.D., A.Y.N., S.M.G., T.J.G., G.A., A.S.T., G.G., D.A.J.; Formal analysis: M.K.A., C.M.S., K.E.Z., A.Y.N.; Investigation: M.K.A., C.M.S., P.K.D., K.E.Z., M.T.D., A.Y.N., S.M.G., T.J.G., G.A., A.S.T.; Resources: G.G.; Data curation: M.K.A., C.M.S., K.E.Z., A.Y.N.; Writing - original draft: M.K.A., C.M.S., D.A.J.; Writing - review & editing: C.M.S., K.E.Z., M.T.D., A.Y.N., G.G., D.A.J.; Visualization: M.K.A., C.M.S.; Supervision: D.A.J.; Project administration: D.A.J.; Funding acquisition: M.K.A., D.A.J.

Funding

This research was supported in-part by a Vanderbilt University Medical Center Integrated Training in Engineering and Diabetes grant (T32DK101003) and Molecular Endocrinology Training Program (METP) grant (5T32DK07563); National Institutes of Health grants (F32DK113689, DK-097392, DK-115620); American Diabetes Association grant (1-17-IBS-024), and a Pilot and Feasibility grant through the Vanderbilt University Medical Center Diabetes Research and Training Center (DK20593) grant (P60-DK-20593). Deposited in PMC for release after 12 months.

Peer review history

The peer review history is available online at https://journals.biologists.com/dev/article-lookup/doi/10.1242/dev.194928

References

Alejandro, E. U., Gregg, B., Wallen, T., Kumusoglu, D., Meister, D., Chen, A., Merrins, M. J., Satin, L. S., Liu, M., Arvan, P. et al. (2014). Maternal diet-induced microRNAs and mTOR underlie beta cell dysfunction in offspring. *J. Clin. Invest.* **124**, 4395-4410. doi:10.1172/JCI74237

Balcazar, N., Sathyamurthy, A., Elghazi, L., Gould, A., Weiss, A., Shiojima, I., Walsh, K. and Bernal-Mizrachi, E. (2009). mTORC1 activation regulates β-cell mass and proliferation by modulation of cyclin D2 synthesis and stability. *J. Biol. Chem.* **284**, 7832-7842. doi:10.1074/jbc.M807458200

Bernal-Mizrachi, E., Wen, W., Stahlhut, S., Welling, C. M. and Permutt, M. A. (2001). Islet β cell expression of constitutively active Akt1/PKBα induces striking hypertrophy, hyperplasia, and hyperinsulinemia. *J. Clin. Invest.* **108**, 1631-1638. doi:10.1172/JCI200113785

Bernal-Mizrachi, E., Fatrai, S., Johnson, J. D., Ohsugi, M., Otani, K., Han, Z., Polonsky, K. S. and Permutt, M. A. (2004). Defective insulin secretion and increased susceptibility to experimental diabetes are induced by reduced Akt activity in pancreatic islet β cells. *J. Clin. Invest.* **114**, 928-936. doi:10.1172/JCI200420016

Castiglioni, S., Leidi, M., Carpanese, E. and Maier, J. A. M. (2013). Extracellular magnesium and in vitro cell differentiation: different behaviour of different cells. *Magnesium Res.* **26**, 24-31. doi:10.1684/mrh.2013.0330

Chen, H., Gu, X., Liu, Y., Wang, J., Wirt, S. E., Bottino, R., Schorle, H., Sage, J. and Kim, S. K. (2011). PDGF signalling controls age-dependent proliferation in pancreatic beta-cells. *Nature* **478**, 349-355. doi:10.1038/nature10502

Cozar-Castellano, I., Takane, K. K., Bottino, R., Balamurugan, A. N. and Stewart, A. F. (2004). Induction of beta-cell proliferation and retinoblastoma protein phosphorylation in rat and human islets using adenovirus-mediated transfer of cyclin-dependent kinase-4 and cyclin D1. *Diabetes* **53**, 149-159. doi:10.2337/diabetes.53.1.149

Dadi, P. K., Vierra, N. C., Ustione, A., Piston, D. W., Colbran, R. J. and Jacobson, D. A. (2014). Inhibition of pancreatic β-cell Ca2+/calmodulin-dependent protein kinase II reduces glucose-stimulated calcium influx and insulin secretion, impairing glucose tolerance. *J. Biol. Chem.* **289**, 12435-12445. doi:10.1074/jbc.M114.562587

Fang, L., Zhan, S., Huang, C., Cheng, X., Lv, X., Si, H. and Li, J. (2013). TRPM7 channel regulates PDGF-BB-induced proliferation of hepatic stellate cells via PI3K and ERK pathways. *Toxicol. Appl. Pharmacol.* **272**, 713-725. doi:10.1016/j.taap.2013.08.009

Garfinkel, L. and Garfinkel, D. (1985). Magnesium regulation of the glycolytic pathway and the enzymes involved. *Magnesium* **4**, 60-72.

Gommers, L. M. M., Hill, T. G., Ashcroft, F. M. and de Baaij, J. H. F. (2019). Low extracellular magnesium does not impair glucose-stimulated insulin secretion. *PLoS ONE* **14**, e0217925. doi:10.1371/journal.pone.0217925

Gu, G., Dubauskaite, J. and Melton, D. A. (2002). Direct evidence for the pancreatic lineage: NGN3+ cells are islet progenitors and are distinct from duct progenitors. *Development* **129**, 2447-2457. doi:10.1242/dev.129.10.2447

Gupta, R. K., Gao, N., Gorski, R. K., White, P., Hardy, O. T., Rafiq, K., Brestelli, J. E., Chen, G., Stoeckert, C. J., Jr and Kaestner, K. H. (2007). Expansion of adult β-cell mass in response to increased metabolic demand is dependent on HNF-4α. *Genes Dev.* **21**, 756-769. doi:10.1101/gad.1535507

Hardy, A. B., Wijesekara, N., Genkin, I., Prentice, K. J., Bhattacharjee, A., Kong, D., Chimienti, F. and Wheeler, M. B. (2012). Effects of high-fat diet feeding on Znt8-null mice: differences between β-cell and global knockout of Znt8. *Am. J. Physiol. Endocrinol. Metab.* **302**, E1084-E1096. doi:10.1152/ajpendo.00448.2011

Harper, J. W., Adami, G. R., Wei, N., Keyomarsi, K. and Elledge, S. J. (1993). The p21 Cdk-interacting protein Cip1 is a potent inhibitor of G1 cyclin-dependent kinases. *Cell* **75**, 805-816. doi:10.1016/0092-8674(93)90499-G

Henley, K. D., Gooding, K. A., Economides, A. N. and Gannon, M. (2012). Inactivation of the dual Bmp/Wnt inhibitor Sostdc1 enhances pancreatic islet function. *Am. J. Physiol. Endocrinol. Metab.* **303**, E752-E761. doi:10.1152/ajpendo.00531.2011

Hogh, K.-L. N., Uy, C. E., Asadi, A., Baker, R. K., Riedel, M. J. and Gray, S. L. (2013). Overexpression of peroxisome proliferator-activated receptor α in pancreatic β-cells improves glucose tolerance in diet-induced obese mice. *Exp. Physiol.* **98**, 564-575. doi:10.1113/expphysiol.2012.068734

Jacobson, D. A., Kuznetsov, A., Lopez, J. P., Kash, S., Ämmälä, C. E. and Philipson, L. H. (2007). Kv2.1 ablation alters glucose-induced islet electrical activity, enhancing insulin secretion. *Cell Metab.* **6**, 229-235. doi:10.1016/j.cmet.2007.07.010

Jeanes, A. I., Wang, P., Moreno-Layseca, P., Paul, N., Cheung, J., Tsang, R., Akhtar, N., Foster, F. M., Brennan, K. and Streuli, C. H. (2012). Specific β-containing integrins exert differential control on proliferation and two-dimensional collective cell migration in mammary epithelial cells. *J. Biol. Chem.* **287**, 24103-24112. doi:10.1074/jbc.M112.360834

Ji, Y., Sun, S., Shrestha, N., Darragh, L. B., Shirakawa, J., Xing, Y., He, Y., Carboneau, B. A., Kim, H., An, D. et al. (2019). Toll-like receptors TLR2 and TLR4 block the replication of pancreatic β cells in diet-induced obesity. *Nat. Immunol.* **20**, 677-686. doi:10.1038/s41590-019-0396-z

Jin, J., Desai, B. N., Navarro, B., Donovan, A., Andrews, N. C. and Clapham, D. E. (2008). Deletion of Trpm7 disrupts embryonic development and thymopoiesis without altering Mg2+ homeostasis. *Science* **322**, 756-760. doi:10.1126/science.1163493

Jin, J., Wu, L.-J., Jun, J., Cheng, X., Xu, H., Andrews, N. C. and Clapham, D. E. (2012). The channel kinase, TRPM7, is required for early embryonic development. *Proc. Natl. Acad. Sci. USA* **109**, E225-E233. doi:10.1073/pnas.1120033109

Kleiner, S., Gomez, D., Megra, B., Na, E., Bhavsar, R., Cavino, K., Xin, Y., Rojas, J., Dominguez-Gutierrez, G., Zambrowicz, B. et al. (2018). Mice harboring the human SLC30A8 R138X loss-of-function mutation have increased insulin secretory capacity. *Proc. Natl. Acad. Sci. USA* **115**, E7642-E7649. doi:10.1073/pnas.1721418115

Li, J., Klughammer, J., Farlik, M., Penz, T., Spittler, A., Barbieux, C., Berishvili, E., Bock, C. and Kubicek, S. (2016a). Single-cell transcriptomes reveal characteristic features of human pancreatic islet cell types. *EMBO Rep.* **17**, 178-187. doi:10.15252/embr.201540946

Li, X., Cheng, K. K. Y., Liu, Z., Yang, J.-K., Wang, B., Jiang, X., Zhou, Y., Hallenborg, P., Hoo, R. L. C., Lam, K. S. L. et al. (2016b). The MDM2-p53-pyruvate carboxylase signalling axis couples mitochondrial metabolism to glucose-stimulated insulin secretion in pancreatic beta-cells. *Nat. Commun.* **7**, 11740. doi:10.1038/ncomms11740

Matsuda, M., Mandarino, L. and DeFronzo, R. A. (1999). Synergistic interaction of magnesium and vanadate on glucose metabolism in diabetic rats. *Metabolism* **48**, 725-731. doi:10.1016/S0026-0495(99)90171-3

Nguemo, F., Semmler, J., Reppel, M. and Hescheler, J. (2014). Modulation of L-type calcium current by intracellular magnesium in differentiating cardiomyocytes derived from induced pluripotent stem cells. *Stem Cells Dev.* **23**, 1316-1327. doi:10.1089/scd.2013.0549

Peng, Z., Aggarwal, R., Zeng, N., He, L., Stiles, E. X., Debebe, A., Chen, J., Chen, C.-Y. and Stiles, B. L. (2020). AKT1 regulates endoplasmic reticulum stress and mediates the adaptive response of pancreatic beta cells. *Mol. Cell. Biol.* **40**, e00031-20. doi:10.1128/MCB.00031-20

Polyak, K., Lee, M.-H., Erdjument-Bromage, H., Koff, A., Roberts, J. M., Tempst, P. and Massagué, J. (1994). Cloning of p27Kip1, a cyclin-dependent kinase inhibitor and a potential mediator of extracellular antimitogenic signals. *Cell* **78**, 59-66. doi:10.1016/0092-8674(94)90572-X

Rachdi, L., Balcazar, N., Elghazi, L., Barker, D. J., Krits, I., Kiyokawa, H. and Bernal-Mizrachi, E. (2006). Differential effects of p27 in regulation of β-cell mass during development, neonatal period, and adult life. *Diabetes* **55**, 3520-3528. doi:10.2337/db06-0861

Rane, S. G., Dubus, P., Mettus, R. V., Galbreath, E. J., Boden, G., Reddy, E. P. and Barbacid, M. (1999). Loss of Cdk4 expression causes insulin-deficient diabetes and Cdk4 activation results in beta-islet cell hyperplasia. *Nat. Genet.* **22**, 44-52. doi:10.1038/8751

Rodriguez-Calvo, T., Zapardiel-Gonzalo, J., Amirian, N., Castillo, E., Lajevardi, Y., Krogvold, L., Dahl-Jørgensen, K. and von Herrath, M. G. (2017). Increase in pancreatic proinsulin and preservation of β-cell mass in autoantibody-positive donors prior to type 1 diabetes onset. *Diabetes* **66**, 1334-1345. doi:10.2337/db16-1343

Roe, M. W., Philipson, L. H., Frangakis, C. J., Kuznetsov, A., Mertz, R. J., Lancaster, M. E., Spencer, B., Worley, J. F., III and Dukes, I. D. (1994). Defective glucose-dependent endoplasmic reticulum Ca2+ sequestration in diabetic mouse islets of Langerhans. *J. Biol. Chem.* **269**, 18279-18282. doi:10.1016/S0021-9258(17)32299-8

Rubin, H. (1975). Central role for magnesium in coordinate control of metabolism and growth in animal cells. *Proc. Natl. Acad. Sci. USA* **72**, 3551-3555. doi:10.1073/pnas.72.9.3551

Rubin, H. (2005a). Magnesium: The missing element in molecular views of cell proliferation control. *BioEssays* **27**, 311-320. doi:10.1002/bies.20183

Rubin, H. (2005b). The membrane, magnesium, mitosis (MMM) model of cell proliferation control. *Magnesium Res.* **18**, 268-274.

Runnels, L. W., Yue, L. and Clapham, D. E. (2001). TRP-PLIK, a bifunctional protein with kinase and ion channel activities. *Science* **291**, 1043-1047. doi:10.1126/science.1058519

Ryazanova, L. V., Rondon, L. J., Zierler, S., Hu, Z., Galli, J., Yamaguchi, T. P., Mazur, A., Fleig, A. and Ryazanov, A. G. (2010). TRPM7 is essential for Mg(2+) homeostasis in mammals. *Nat. Commun.* **1**, 109. doi:10.1038/ncomms1108

Sahni, J. and Scharenberg, A. M. (2008). TRPM7 ion channels are required for sustained phosphoinositide 3-kinase signaling in lymphocytes. *Cell Metab.* **8**, 84-93. doi:10.1016/j.cmet.2008.06.002

Sahni, J., Tamura, R., Sweet, I. R. and Scharenberg, A. M. (2010). TRPM7 regulates quiescent/proliferative metabolic transitions in lymphocytes. *Cell Cycle* **9**, 3565-3574. doi:10.4161/cc.9.17.12798

Schmitz, C., Perraud, A.-L., Johnson, C. O., Inabe, K., Smith, M. K., Penner, R., Kurosaki, T., Fleig, A. and Scharenberg, A. M. (2003). Regulation of vertebrate cellular Mg2+ homeostasis by TRPM7. *Cell* **114**, 191-200. doi:10.1016/S0092-8674(03)00556-7

Sgambato, A., Wolf, F. I., Faraglia, B. and Cittadini, A. (1999). Magnesium depletion causes growth inhibition, reduced expression of cyclin D1, and increased expression of P27Kip1 in normal but not in transformed mammary epithelial cells. *J. Cell. Physiol.* **180**, 245-254. doi:10.1002/(SICI)1097-4652(199908)180:2<245::AID-JCP12>3.0.CO;2-R

Stanger, B. Z., Tanaka, A. J. and Melton, D. A. (2007). Organ size is limited by the number of embryonic progenitor cells in the pancreas but not the liver. *Nature* **445**, 886-891. doi:10.1038/nature05537

Tani, D., Monteilh-Zoller, M. K., Fleig, A. and Penner, R. (2007). Cell cycle-dependent regulation of store-operated I(CRAC) and Mg2+-nucleotide-regulated MagNuM (TRPM7) currents. *Cell Calcium* **41**, 249-260. doi:10.1016/j.ceca.2006.07.004

Thorens, B., Tarussio, D., Maestro, M. A., Rovira, M., Heikkilä, E. and Ferrer, J. (2015). Ins1(Cre) knock-in mice for beta cell-specific gene recombination. *Diabetologia* **58**, 558-565. doi:10.1007/s00125-014-3468-5

Tuttle, R. L., Gill, N. S., Pugh, W., Lee, J.-P., Koeberlein, B., Furth, E. E., Polonsky, K. S., Naji, A. and Birnbaum, M. J. (2001). Regulation of pancreatic β-cell growth and survival by the serine/threonine protein kinase Akt1/PKBα. *Nat. Med.* **7**, 1133-1137. doi:10.1038/nm1001-1133

Vierra, N. C., Dadi, P. K., Jeong, I., Dickerson, M., Powell, D. R. and Jacobson, D. A. (2015). Type 2 diabetes-associated K+ channel TALK-1 modulates beta-cell electrical excitability, second-phase insulin secretion, and glucose homeostasis. *Diabetes* **64**, 3818-3828. doi:10.2337/db15-0280

Vierra, N. C., Dadi, P. K., Milian, S. C., Dickerson, M. T., Jordan, K. L., Gilon, P. and Jacobson, D. A. (2017). TALK-1 channels control beta cell endoplasmic reticulum Ca2+ homeostasis. *Sci. Signal.* **10**, eaan2883. doi:10.1126/scisignal.aan2883

Wang, S., Yan, J., Anderson, D. A., Xu, Y., Kanal, M. C., Cao, Z., Wright, C. V. and Gu, G. (2010). Neurog3 gene dosage regulates allocation of endocrine and exocrine cell fates in the developing mouse pancreas. *Dev. Biol.* **339**, 26-37. doi:10.1016/j.ydbio.2009.12.009

Wicksteed, B., Brissova, M., Yan, W., Opland, D. M., Plank, J. L., Reinert, R. B., Dickson, L. M., Tamarina, N. A., Philipson, L. H., Shostak, A. et al. (2010). Conditional gene targeting in mouse pancreatic ss-Cells: analysis of ectopic Cre transgene expression in the brain. *Diabetes* **59**, 3090-3098. doi:10.2337/db10-0624

Wimhurst, J. M. and Manchester, K. L. (1972). Comparison of ability of Mg and Mn to activate the key enzymes of glycolysis. *FEBS Lett.* **27**, 321-326. doi:10.1016/0014-5793(72)80650-1

Yee, N. S., Lorent, K. and Pack, M. (2005). Exocrine pancreas development in zebrafish. *Dev. Biol.* **284**, 84-101. doi:10.1016/j.ydbio.2005.04.035

Yee, N. S., Zhou, W. and Liang, I.-C. (2011). Transient receptor potential ion channel Trpm7 regulates exocrine pancreatic epithelial proliferation by Mg2+-sensitive Socs3a signaling in development and cancer. *Dis. Model. Mech.* **4**, 240-254. doi:10.1242/dmm.004564

Yu, Y., Chen, S., Xiao, C., Jia, Y., Guo, J., Jiang, J. and Liu, P. (2014). TRPM7 is involved in angiotensin II induced cardiac fibrosis development by mediating calcium and magnesium influx. *Cell Calcium* **55**, 252-260. doi:10.1016/j.ceca.2014.02.019

Zhang, X., Gaspard, J. P., Mizukami, Y., Li, J., Graeme-Cook, F. and Chung, D. C. (2005). Overexpression of cyclin D1 in pancreatic β-cells in vivo results in islet hyperplasia without hypoglycemia. *Diabetes* **54**, 712-719. doi:10.2337/diabetes.54.3.712

Zierler, S., Hampe, S. and Nadolni, W. (2017). TRPM channels as potential therapeutic targets against pro-inflammatory diseases. *Cell Calcium* **67**, 105-115. doi:10.1016/j.ceca.2017.05.002

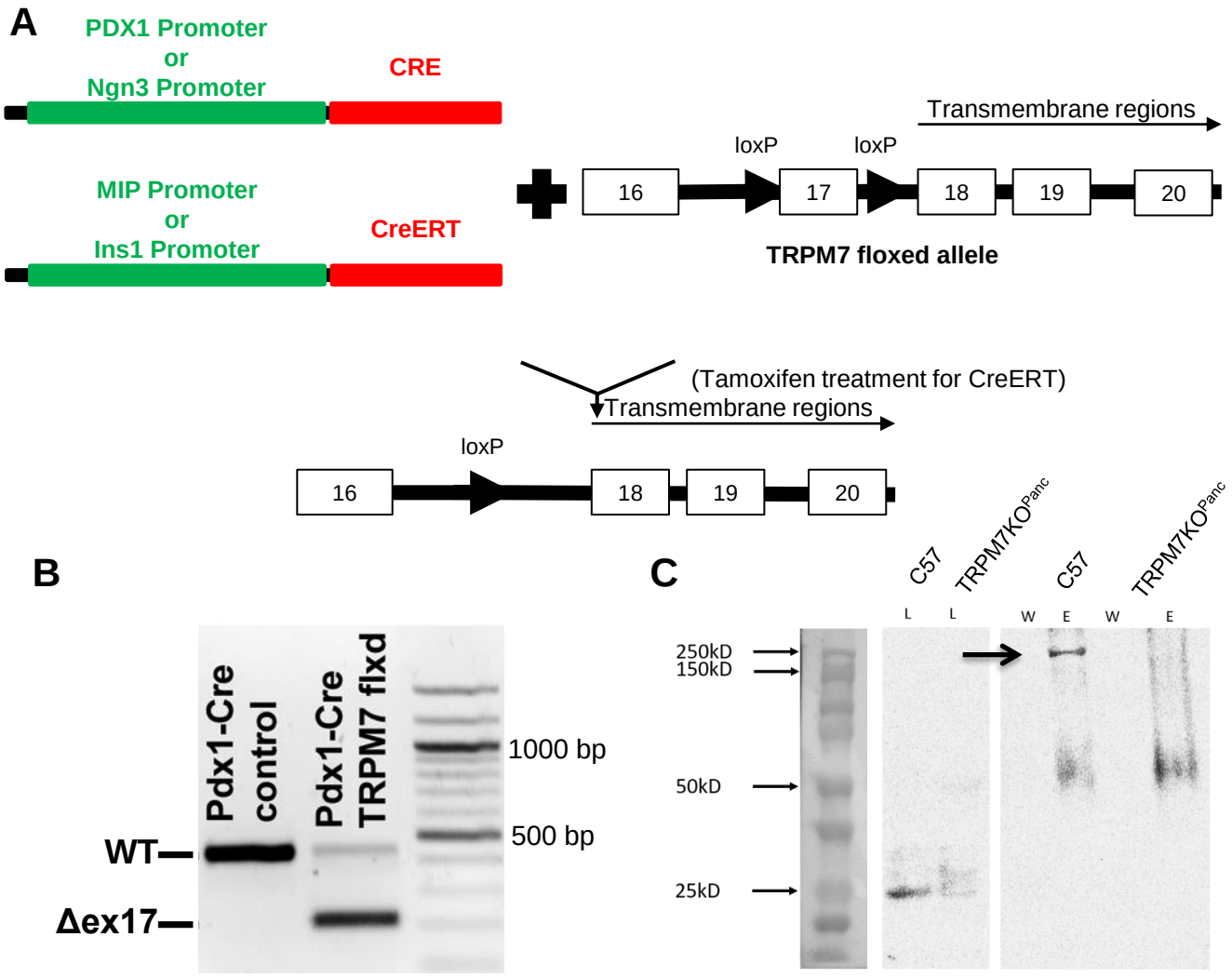

Fig. S1. Mouse model design and confirmation of successful PDX knockout.(A) Schematic of the transgenic design of mouse models with chronic (TRPM7KO^{Panc} or TRPM7KO^{Endo}) pancreatic specific and conditional β-cell specific tamoxifen-inducible (TRPM7KO^{MIPβ} or TRPM7KO^{Insβ}) TRPM7 ablation. (B) Islet genomic DNA from Pdx1-Cre or TRPM7KO^{Panc} mice analyzed by PCR for TRPM7 exon 17 deletion. (C) Immunoprecipitation showing knockdown of TRPM7 protein in whole cell lysate from C57/B6 (C57) or TRPM7KO^{Panc} mouse pancreas from 12-week animals. Black arrow indicates band associated with full length TRPM7 protein. L = load, W = wash, E = elution.

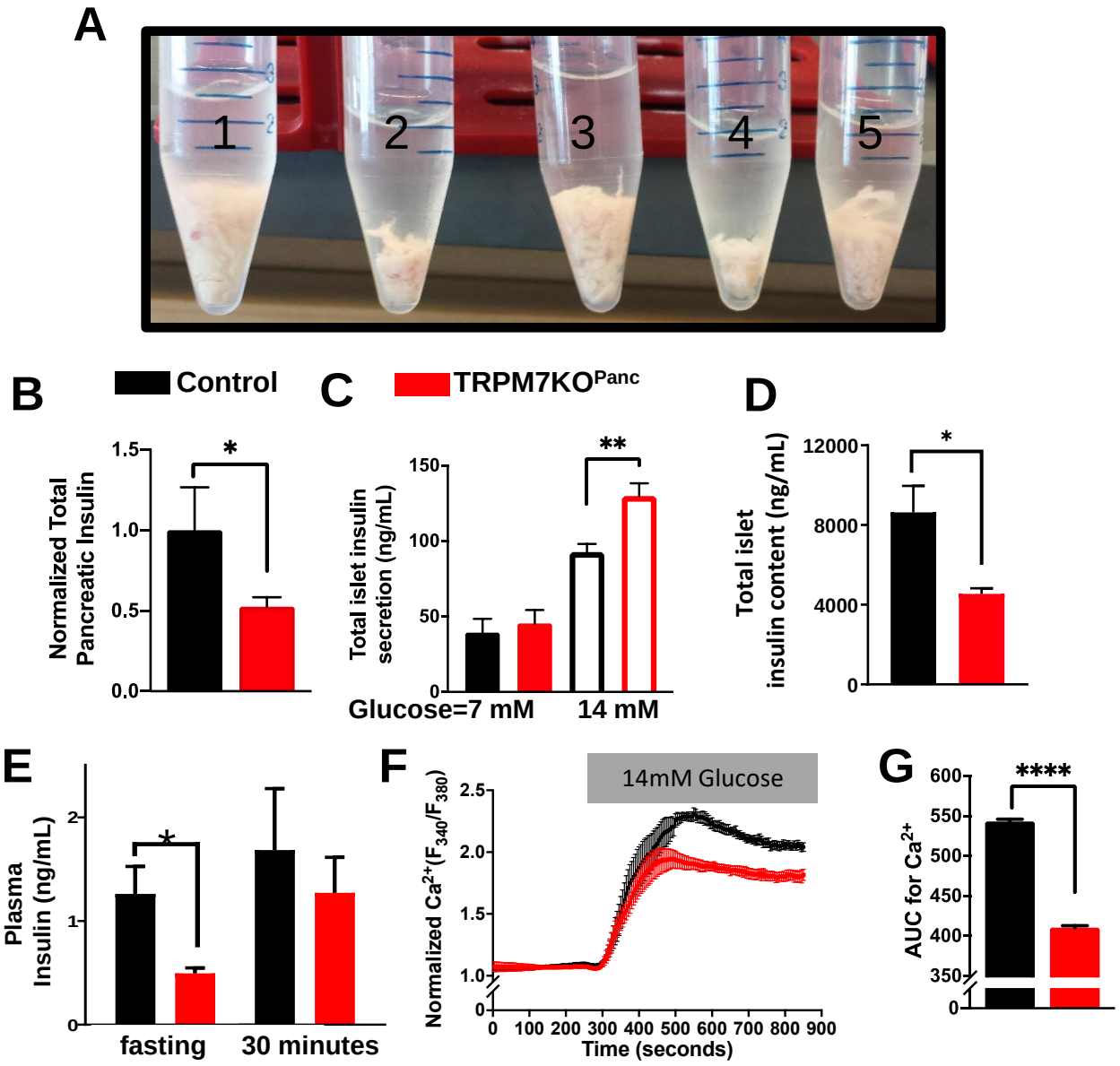

Fig. S2. Adult TRPM7KO^{Panc} pancreata showed diminished size and insulin content. (A) Pancreata harvested from TRPM7KO^{Panc} mice (2, 4) following distention appeared significantly smaller than those from control mice (1, 3, 5). (B) Total pancreatic insulin was significantly lower in TRPM7KO^{Panc} mice compared to controls (47.39 ± 15.75% reduction, n = 3 P<0.05). (C) GSIS was significantly increased in TRPM7KO^{Panc} mice compared to control (39.95 ± 10.69%, n = 5). *(D) Total islet insulin content was reduced in* TRPM7KO^{Panc} islets compared to controls (n= *3* mice each and 20 equivalent sized islets/mouse) (E) Fasting plasma insulin was reduced in TRPM7KO^{Panc} mice, but 30 minutes post GTT glucose bolus plasma insulin was equivalent between TRPM7KO^{Panc} mice and controls. Relative glucose-stimulated (14 mM) cytosolic Ca^{2+} responses (F) and total AUC (G) in control (black) and TRPM7KO^{Panc} (red) islets. Where applicable analysis are mean ± SEM. *P<0.05, **P<0.01, ****P<0.0001.

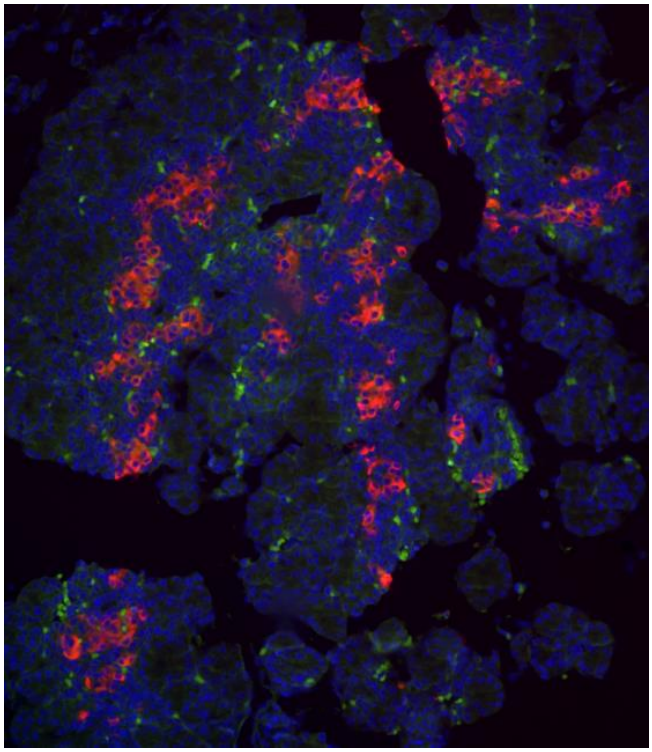

Fig. S3. Cre expression in E16.5 TRPM7KO^{Endo} mice. Representative immunofluorescent image of pancreatic section from TRPM7KO^{Endo} mouse (Cre -green, insulin - red) from a E16.5 pancreatic section.

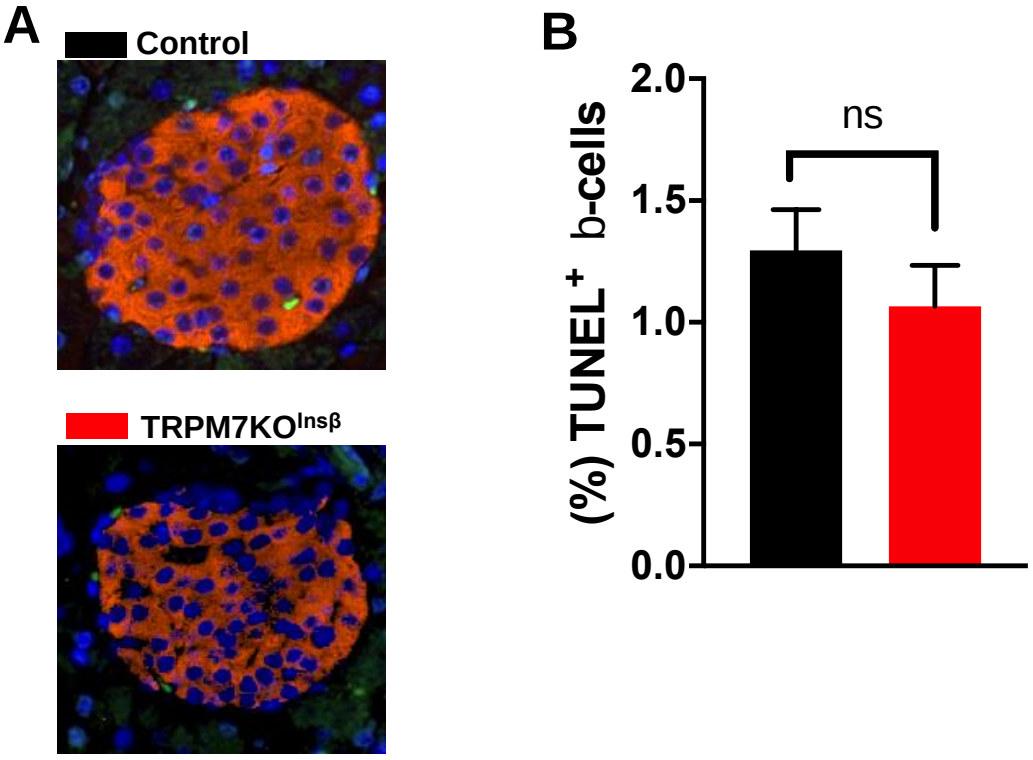

Fig. S4. β-cell specific ablation of TRPM7 (TRPM7KO$^{Ins\beta}$) did not affect apoptosis (HFD). Representative images of pancreas sections immunostained for insulin (red), TUNEL (green) and DAPI (blue) from control and TRPM7KO$^{Ins\beta}$ mice. (B) Percentage of TUNEL^{+} β-cells (*n=3, P=0.385*). Where applicable analysis are mean ± SEM.

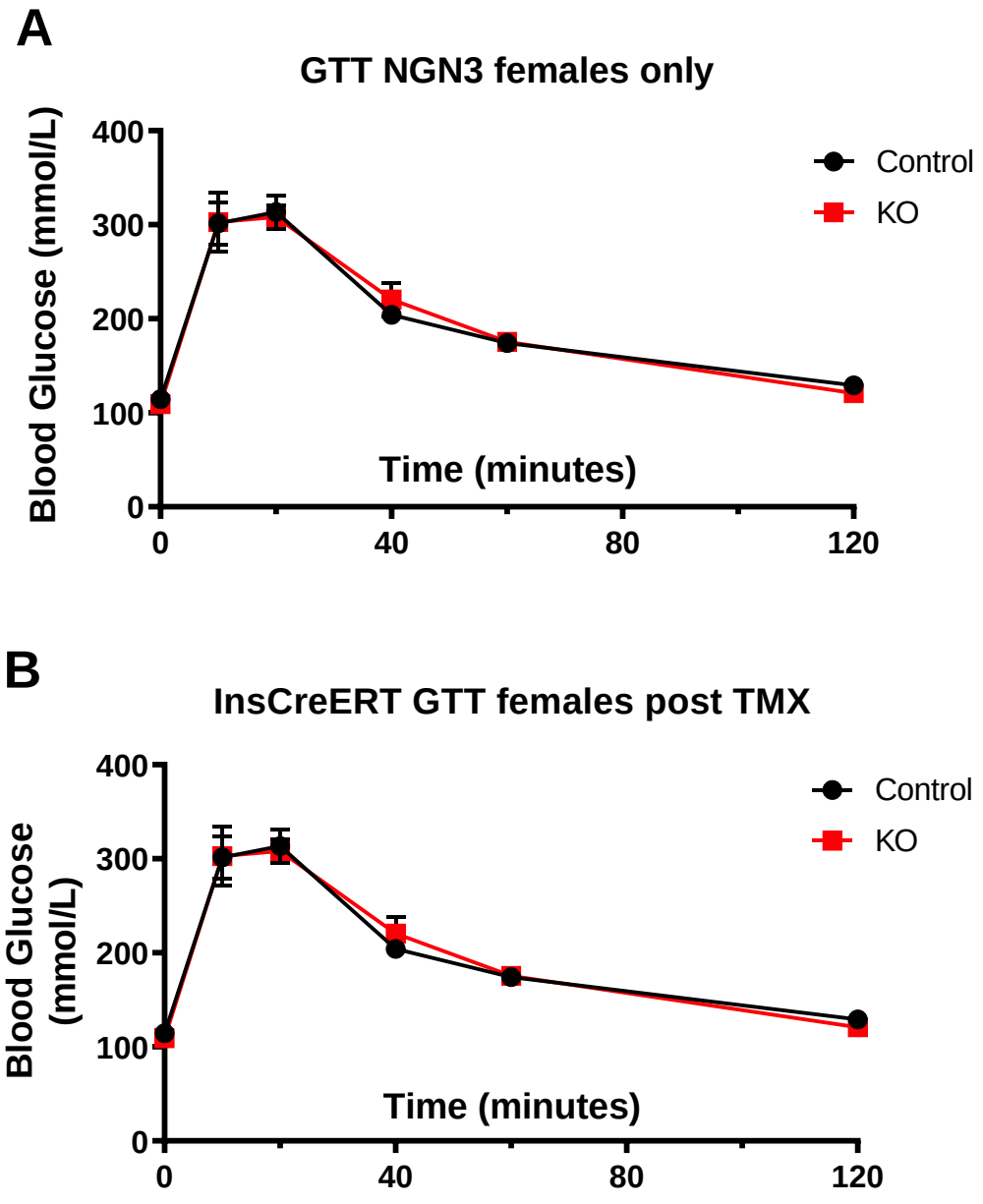

Fig. S5. Female TRPM7KO^{Endo} and TRPM7KO^{INSβ} show normal glucose tolerance. Glucose tolerance of 12-week-old female TRPM7KO^{Endo} (A) and TRPM7KO^{INSβ} (B) mice compared to controls. TRPM7KO^{INSβ} mice and their controls were treated with tamoxifen and allowed 2 weeks recovery post tamoxifen before GTT.

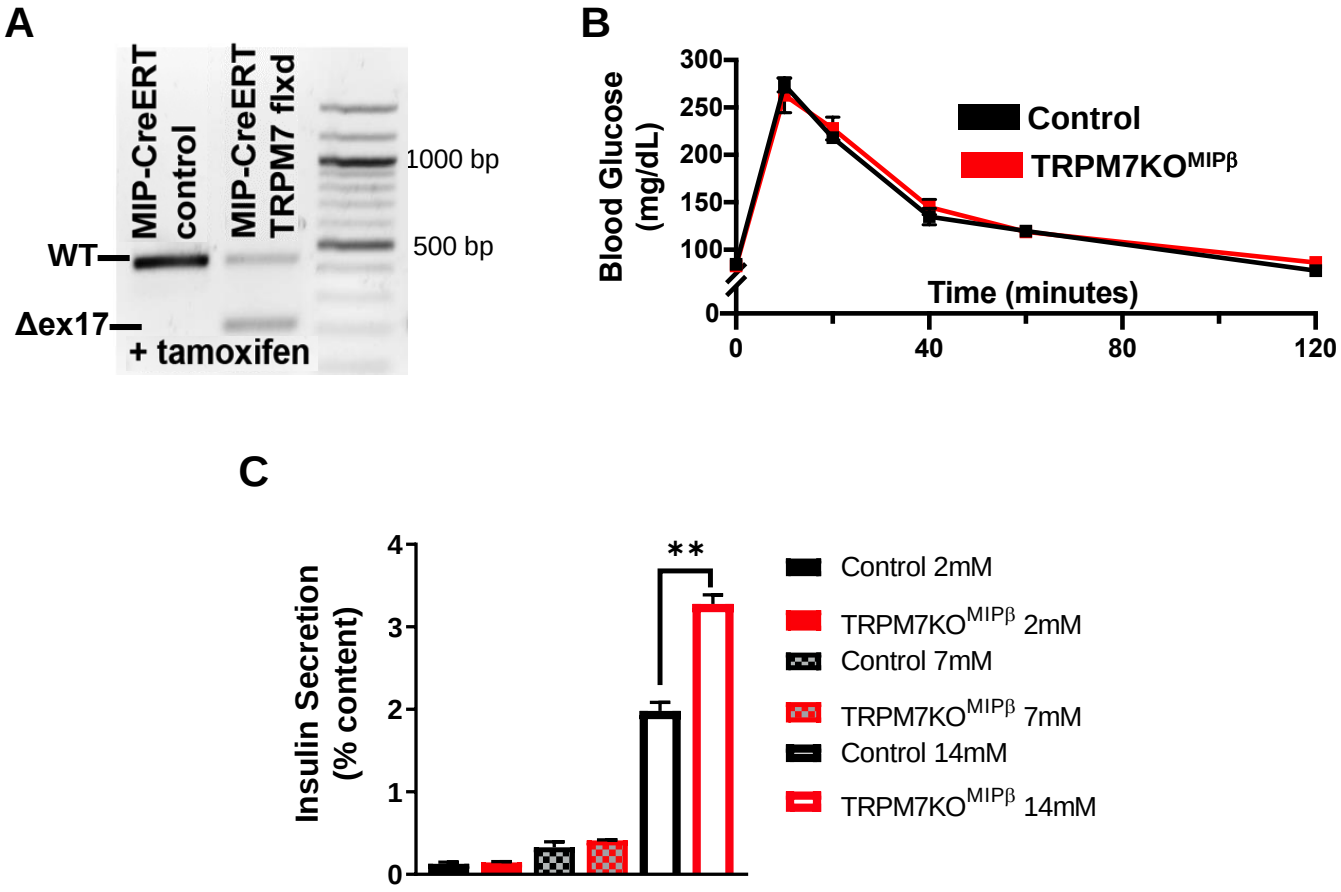

Fig. S6. β-cell knockdown of TRPM7 (TRPM7KO$^{MIP\beta}$) enhances GSIS but not GTT. (A) Islet genomic DNA from MIP-CreERT or TRPM7KO$^{MIP\beta}$ mice analyzed by PCR for TRPM7 exon 17 deletion post-tamoxifen treatment. (B) Glucose tolerance from 12-week-old MIP-CreERT and TRPM7KO$^{MIP\beta}$ males (n= 5 each). (C) Insulin secretion from TRPM7KO$^{MIP\beta}$ islets compared to controls normalized to content. Where applicable analysis are mean ± SEM. $^{**}P<0.01$.

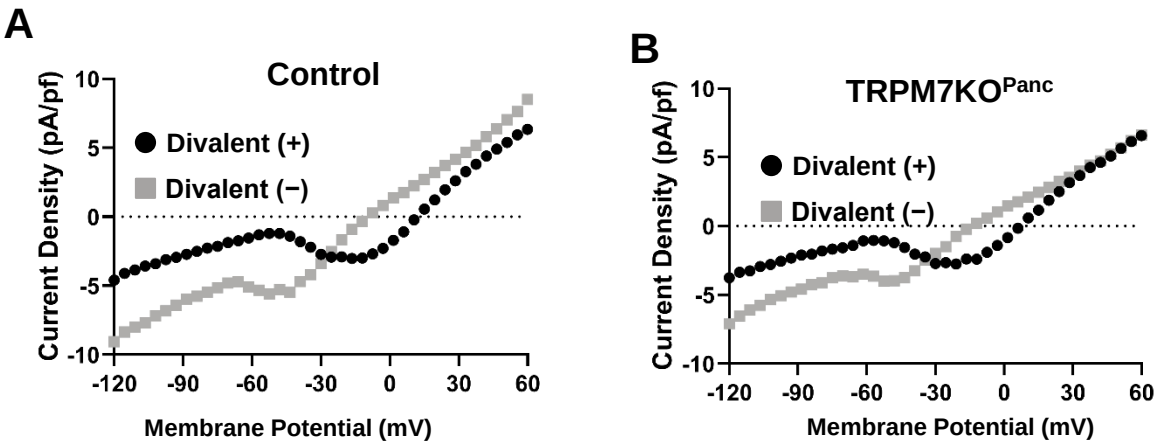

Fig. S7. TRPM7 alters β-cell whole cell currents. Representative TRPM7 currents recorded from control (A) and TRPM7KO^{Panc} (B) β-cells in the presence (black circles) or absence (grey squares) of divalent cations. Data analysis for these recordings can be found in Figure 4A.

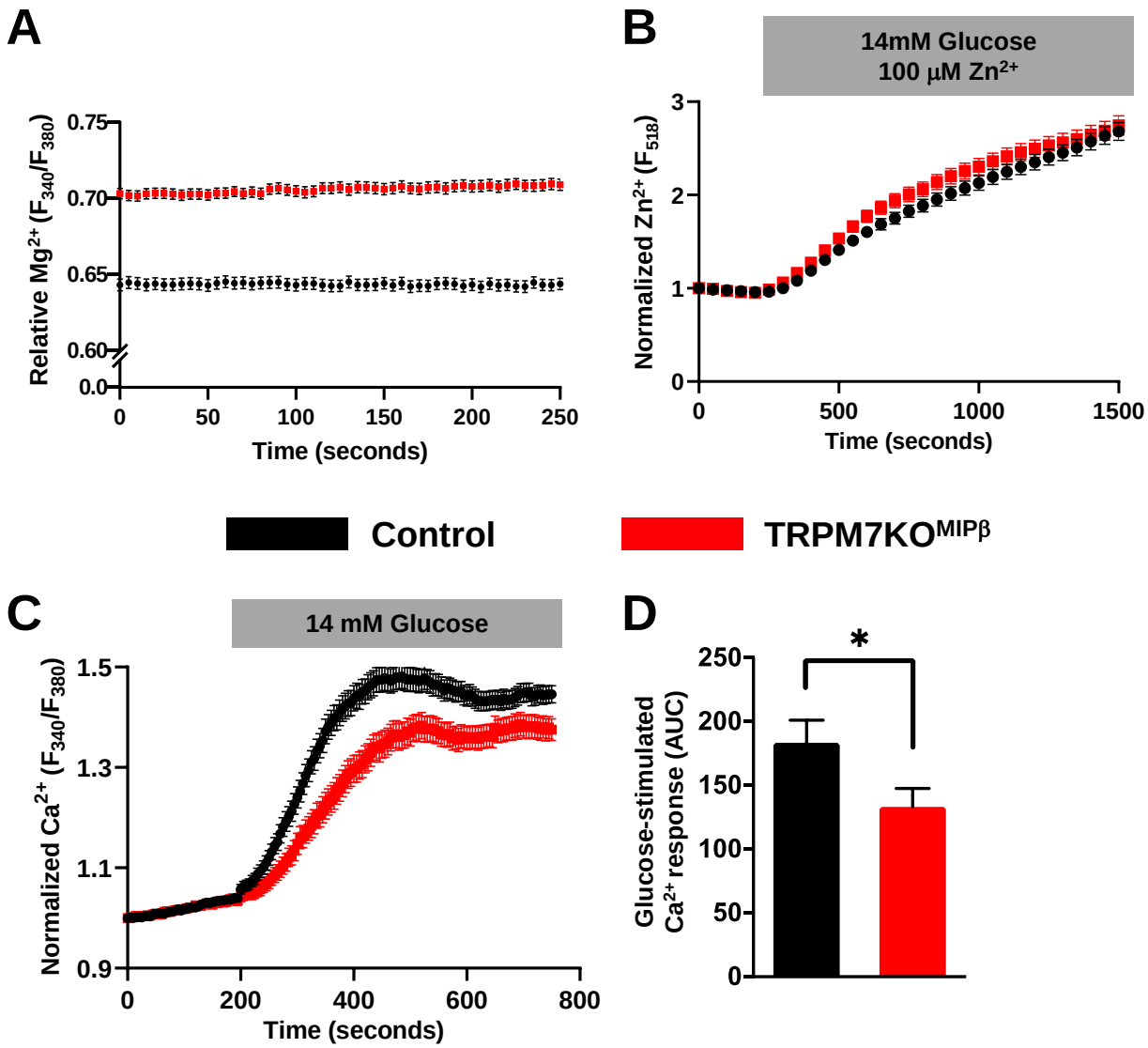

Fig. S8. β-cell specific ablation of TRPM7 (TRPM7KO^{MIPβ}) decreases Ca^{2+} influx and Mg^{2+} efflux. (A) Relative intracellular Mg^{2+} levels in β-cells from control (black) and TRPM7KO^{MIPβ} (red) in the absence of extracellular Mg^{2+}. (B) Relative β-cell intracellular Zn^{2+} levels from TRPM7KO^{MIPβ} and control mice after in response to 100 μM Zn^{2+} and 14 mM glucose (grey bar). (C) Glucose-stimulated (14 mM) islet Ca^{2+} responses and corresponding total AUC (D, 24.21 ± 10.91% reduction, $P<0.05$) from control and TRPM7KO^{MIPβ} mice. Where applicable, data are mean ± SEM and significance is calculated with a two-tailed Student's *t*-test. *$P<0.05$.

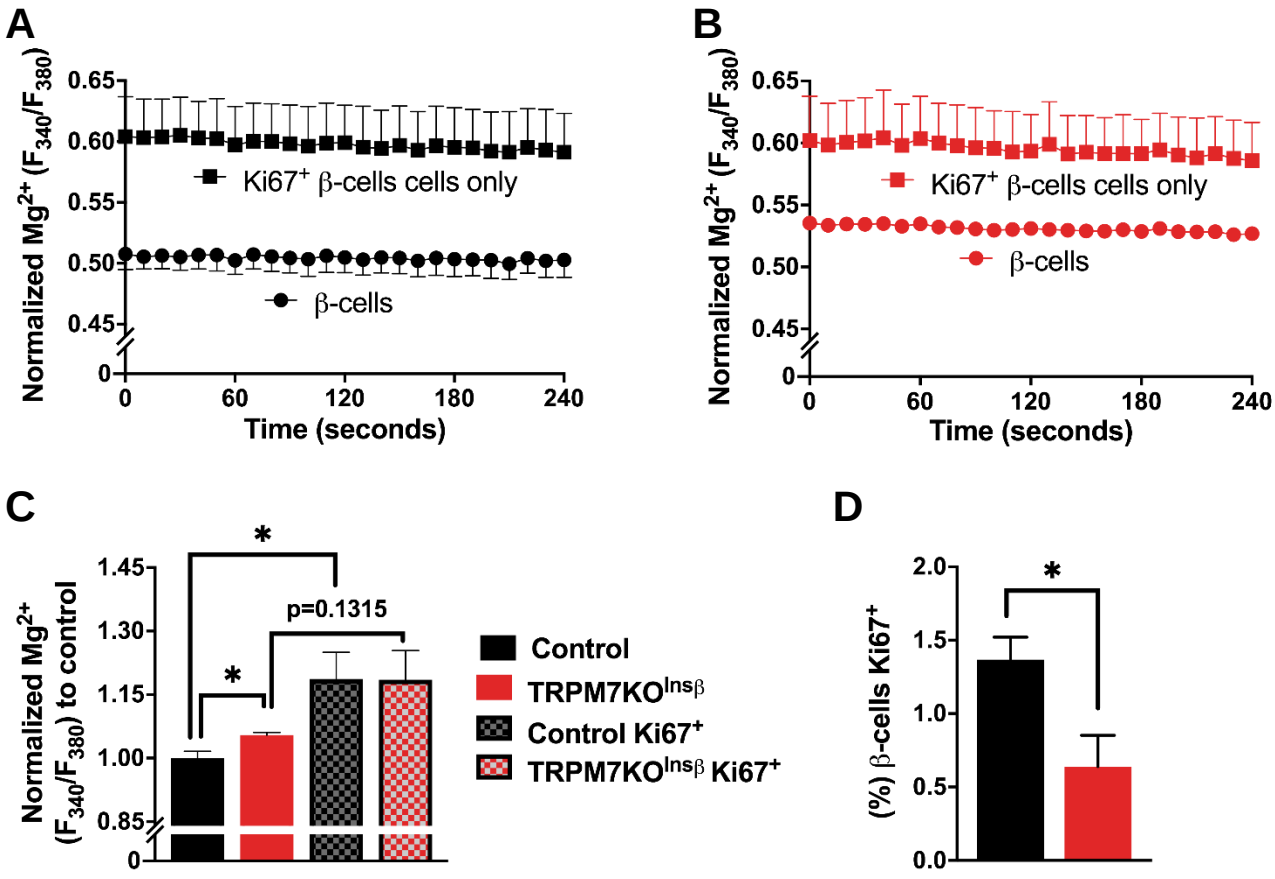

Fig. S9. TRPM7 lowers Mg^{2+} levels within nonproliferating single β-cells as well as β-cells with islet cell clusters. β-cell Mg^{2+} levels recorded from non-proliferating(●) and proliferating(■) cells; the β-cell were from control (A) and TRPM7KO$^{Ins\beta}$ (B) mice 2 weeks post exposure to HFD. Note: this data combines Mg^{2+} levels from both single β-cells and from those within islet cell clusters. (C) Fold change in Mg^{2+} levels for the indicated β-cell cohorts normalized to non-proliferating controls (β-cells from islets of animals fed a HFD for 2-weeks). (D) Percent of Ki67-positive β-cells from cohorts shown in A and B. Data are mean±SEM, *P<0.05.